Acta Mech 219, 309–335 (2011)
DOI 10.1007/s00707-011-0459-1

A. R. Saidi · A. Hasani Baferani · E. Jomehzadeh

Benchmark solution for free vibration of functionally graded moderately thick annular sector plates

Received: 5 May 2010 / Revised: 20 January 2011 / Published online: 23 February 2011
© Springer-Verlag 2011

Abstract In the present article, an exact analytical solution for free vibration analysis of a moderately thick functionally graded (FG) annular sector plate is presented. Based on the first-order shear deformation plate theory, five coupled partial differential equations of motion are obtained without any simplification. Doing some mathematical manipulations, these highly coupled equations are converted into a sixth-order and a fourth-order decoupled partial differential equation. The decoupled equation are solved analytically for an FG annular sector plate with simply supported radial edges. The accurate natural frequencies of the FG annular sector plates with nine different boundary conditions are presented for several aspect ratios, some thickness/length ratios, different sector angles, and various power law indices. The results show that variations of the thickness, aspect ratio, sector angle, and boundary condition of the FG annular sector plates can change the vibration wave number. Also for an FG annular sector plate with one free edge, in opposite to the other boundary conditions, the natural frequency decreases with increasing the aspect ratio for small aspect ratios. Moreover, the mode shape contour plots are depicted for an FG annular sector plate with various boundary conditions. The accurate natural frequencies of FG annular sector plates are presented for the first time and can serve as a benchmark solution.

1 Introduction

Since sector plates combine light weight and form efficiency with high load-carrying capacity, economy, and technological effectiveness, they are important parts inside many structures and are extensively used in all fields of engineering such as architectural structures, bridges, hydraulic structures, containers, airplanes, missiles, ships, and instruments. Due to their widespread use, it is essential to understand the dynamic behavior of such plates.

Functionally graded materials (FGM's) are microscopically inhomogeneous in which their mechanical properties vary smoothly and continuously from one surface to the other. The concept of functionally graded materials was proposed in 1984 by the material scientists in the Sendai area of Japan [1]. This is achieved by gradually varying the volume fraction of the material constituents. Typically, these materials are made from a mixture of ceramics and metal [2].

Many studies on free vibration analysis of homogenous annular sector plates are available in the literature. Srinivasan and Thiruvekatachari [3] presented a numerical method for the free vibration of polar orthotropic clamped annular sector plates by using first-order shear deformation plate theory. Cheung and Kwok [4] studied the free vibration analysis of circular and sector thick, layered plates with curved boundaries by using the finite element method. Mizusawa [5] developed the free vibration of Mindlin annular sector plates with simply

A. R. Saidi (✉) · A. H. Baferani · E. Jomehzadeh
Department of Mechanical Engineering, Shahid Bahonar University of Kerman, Kerman, Iran
E-mail: saidi@mail.uk.ac.ir
Tel.: +98-341-2111763
Fax: +98-341-2120964

supported straight edges by using the finite strip and the finite prism methods. By using the Rayleigh-Ritz procedure, Xiang et al. [6] investigated the free vibration of thick sector plates with different supporting edge conditions. The fundamental frequency has been reported for completely free sectorial plates using the Ritz method by McGee et al. [7]. Also, McGee et al. [8] presented the comprehensive exact solutions for free vibrations of thick annular sectorial plates with simply supported radial edges. They presented exact results for homogenous isotropic annular sector plates under different boundary conditions. Based on the Mindlin theory, Huang et al. [9] studied exact analytical solutions for free vibrations of thick complete sectorial plates with simply supported radial edges. By using the differential quadrature element method (DQM), Liew and Liu [10] investigated the free vibration analysis of moderately thick annular sector plates based on first-order shear deformation theory. Wang and Wang [11] studied the free vibration analysis of thin sector plates by a new version of DQM. Yongqiang and Jian [12] investigated the free vibration analysis of circular and annular sectorial thin plates using curve strip Fourier p-elements. Chen and Ding [13] investigated the free vibration of a functionally graded piezoelectric plate based on the three-dimensional elasticity theory. Zhou et al. [14] studied the three-dimensional vibration analysis of annular sector plates with various boundary conditions using the Chebyshev–Ritz method. Based on the first-order shear deformation theory, Jomehzadeh and Saidi [15,16] presented an analytical solution for the free vibration of transversely isotropic complete sector and annular sector plates.

Srinivasan and Thiruvekatachari [17], by using an integral equation technique, studied the free vibration analysis of laminated annular sector plates with clamped edges. Based on the third-order shear deformation plate theory, Atashipour et al. [18] presented an analytical solution for the bending analysis of thick annular sector plates and studied the effect of the boundary layer phenomenon. By using the Frobenius method, Huang and Ho [19] studied an analytical solution for free vibrations of a polarly orthotropic Mindlin sectorial plate with simply supported radial edges. Based on Chebyshev polynomials, Sharma et al. [20] presented a simple analytical formulation for the eigenvalue problem of buckling and free vibration analysis of shear deformable laminated sector plates made up of cylindrically orthotropic layers. Nosier et al. [21] studied the effect of a boundary layer phenomenon in laminated circular sector plates based on the Mindlin-Reissner plate theory. Malekzadeh [22] investigated three-dimensional free vibration of thick laminated annular sector plates with simply supported radial edges and arbitrary boundary conditions on the circular edges using a hybrid method. Malekzadeh et al. [23] presented a three-dimensional hybrid numerical method to study the dynamic response of thick laminated annular sector plates with simply supported radial edges subjected to a radially distributed line load, which moves along the circumferential direction. Also, Malekzadeh et al. [24] studied the three-dimensional layer-wise finite element free vibration analysis of thick laminated annular plates on an elastic foundation.

Although many studies have been carried out for the vibration analysis of homogeneous isotropic and laminated sector plates, a few articles can be found on the vibration analysis of a functionally graded sector plates that are all done using DQM. Nie and Zhong [25] presented the free and forced vibration analysis of FG annular sectorial plates with simply supported radial edges by means of DQM. Hosseini-Hashemi et al. [26] studied the buckling and free vibration behaviors of radially functionally graded circular and annular sector thin plates subjected to uniform in-plane compressive loads and resting on the Pasternak elastic foundation using DQM. Also, Hosseini-Hashemi et al. [27] presented the vibration analysis of radially FG sectorial plates of variable thickness on elastic foundations by using DQM.

To the best of the authors' knowledge, the exact solutions for the free vibration of FG annular sector plates have not been presented in the literature, yet. In the present article, the free vibration analysis of a functionally graded annular sector plate is analytically investigated. The material properties are assumed to vary through the thickness which makes the problem more complicated due to the coupling between in-plane and out of plane governing equations of motion. Five highly coupled partial differential equations of motion are obtained based on the first-order shear deformation plate theory. Some mathematical manipulations are used to decouple these equations. For solving the decoupled equations, it is assumed that the FG annular sector plate has simply supported radial edges and arbitrary boundary conditions along the circular edges. By satisfying boundary conditions at the inner and outer radii, an eigenvalue problem for finding the natural frequency is obtained. The non-dimensional natural frequencies are tabulated for FG sector plates with all nine different boundary conditions along the circular edges. The benchmark natural frequencies of the FG annular sector plate are presented with several aspect ratios, some thickness/length ratios, different sector angle, and various power law indices.

2 Formulations

Consider an FG annular sector plate with inner radius a, outer radius b, uniform thickness h and sector angle β (Fig. 1). Considering the displacement components of the first-order shear deformation plate theory and using

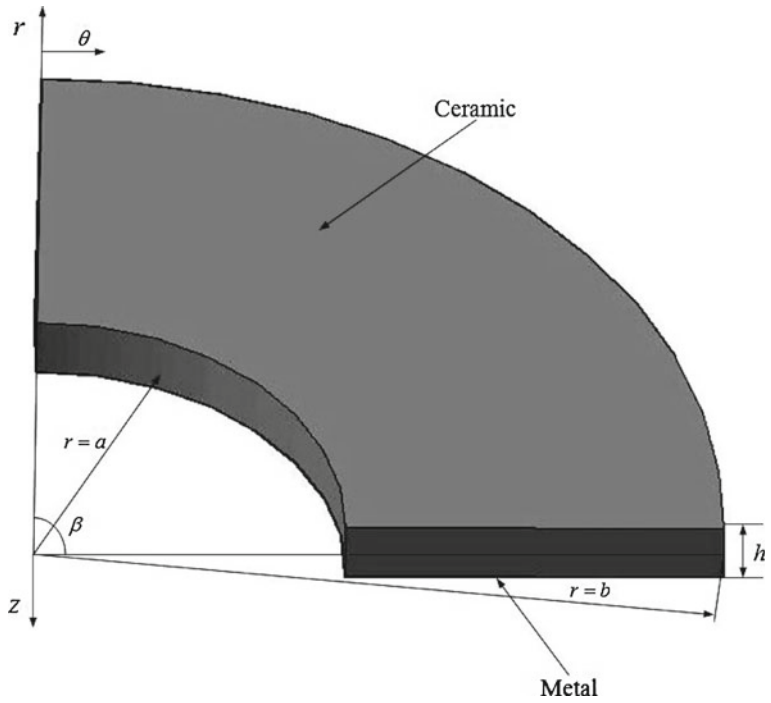

Fig. 1 Geometry and coordinate system of an annular sector plate

Hamilton's principle for an FG annular sector plate, the governing equations of motion can be obtained as [28]

$$\begin{aligned}
&\frac{\partial N_{rr}}{\partial r}+\frac{1}{r}\frac{\partial N_{r\theta}}{\partial \theta}+\frac{N_{rr}-N_{\theta\theta}}{r}=I_0\ddot{u}_1+I_1\ddot{\psi}_r,\\
&\frac{\partial N_{r\theta}}{\partial r}+\frac{1}{r}\frac{\partial N_{\theta\theta}}{\partial \theta}+\frac{2N_{r\theta}}{r}=I_0\ddot{u}_2+I_1\ddot{\psi}_\theta,\\
&\frac{\partial M_{rr}}{\partial r}+\frac{1}{r}\frac{\partial M_{r\theta}}{\partial \theta}+\frac{M_{rr}-M_{\theta\theta}}{r}-Q_r=I_1\ddot{u}_1+I_2\ddot{\psi}_r,\\
&\frac{\partial M_{r\theta}}{\partial r}+\frac{1}{r}\frac{\partial M_{\theta\theta}}{\partial \theta}+\frac{2M_{r\theta}}{r}-Q_\theta=I_1\ddot{u}_2+I_2\ddot{\psi}_\theta,\\
&\frac{\partial Q_r}{\partial r}+\frac{1}{r}\frac{\partial Q_\theta}{\partial \theta}+\frac{Q_r}{r}=I_0\ddot{u}_3.
\end{aligned} \tag{1}$$

In the above equations, a dot above each parameter denotes partial differentiation with respect to time ($\dot{()}=\partial()/\partial t$). The parameters u_1, u_2, and u_3 are the displacement components in r, θ, and z directions, respectively, ψ_r and ψ_θ are the rotation functions of the middle surface. Also, N_{rr}, $N_{\theta\theta}$, and $N_{r\theta}$ are in-plane resultant forces, M_{rr}, $M_{\theta\theta}$, and $M_{r\theta}$ are the bending and twisting moment intensities, Q_r and Q_θ are the out of plane resultant forces, and $I_t(t=0,1,2)$ are the inertia terms which are defined as

$$(N_{rr}, N_{\theta\theta}, N_{r\theta})=\int_{-h/2}^{h/2}(\sigma_{rr}, \sigma_{\theta\theta}, \quad \sigma_{r\theta})\,\mathrm{d}z,$$

$$(M_{rr}, M_{\theta\theta}, M_{r\theta})=\int_{-h/2}^{h/2}(\sigma_{rr}, \sigma_{\theta\theta}, \sigma_{r\theta})\,z\mathrm{d}z,$$

$$(Q_r, Q_\theta) = k^2 \int_{-h/2}^{h/2} (\sigma_{rz}, \sigma_{\theta z})\, \mathrm{d}z,$$

$$(I_0, I_1, I_2) = \int_{-h/2}^{h/2} \rho(z)\left(1, z, z^2\right) \mathrm{d}z \tag{2}$$

where k^2 is the shear correction factor which is assumed to be $\pi^2/12$. Also σ_{rr}, $\sigma_{\theta\theta}$, and $\sigma_{r\theta}$, $\sigma_{\theta z}$, σ_{rz} are the normal and shear stress components, respectively. Considering the plane stress state, the stress components of an FG annular sector plate are defined as

$$\begin{aligned}
&\sigma_{rr} = \frac{E(z)}{1-\nu^2}\left(\varepsilon_{rr} + \nu\varepsilon_{\theta\theta}\right), \quad \sigma_{\theta\theta} = \frac{E(z)}{1-\nu^2}\left(\varepsilon_{\theta\theta} + \nu\varepsilon_{rr}\right), \quad \sigma_{r\theta} = \frac{E(z)}{2(1+\nu)}\left(2\varepsilon_{r\theta}\right), \\
&\sigma_{\theta z} = \frac{E(z)}{2(1+\nu)}\left(2\varepsilon_{\theta z}\right), \quad \sigma_{rz} = \frac{E(z)}{2(1+\nu)}\left(2\varepsilon_{rz}\right)
\end{aligned} \tag{3}$$

where ε_{rr} and $\varepsilon_{\theta\theta}$ are the normal strain and $\varepsilon_{r\theta}$, $\varepsilon_{\theta z}$, and ε_{rz} are the shear strain components. Also, $E(z)$ and $\rho(z)$ are, respectively, the Young's modulus and density of the functionally graded material which are assumed to vary through the thickness of the FG plate in z direction, $(-h/2 \le z \le h/2)$ by a power law function as

$$\begin{aligned}
E(z) &= E_m + (E_c - E_m)\left(\frac{1}{2} - \frac{z}{h}\right)^n, \\
\rho(z) &= \rho_m + (\rho_c - \rho_m)\left(\frac{1}{2} - \frac{z}{h}\right)^n
\end{aligned} \tag{4}$$

where n is the power law index of the functionally graded material. The subscripts m and c refer to the metal and ceramic, respectively. By substituting Eqs. (3) into (2) and expressing the strain components in terms of displacement components, the following relations for resultant forces and moments can be obtained:

$$\begin{aligned}
N_{rr} &= A_{11}\frac{\partial u_1}{\partial r} + A_{12}\left(\frac{u_1}{r} + \frac{1}{r}\frac{\partial u_2}{\partial\theta}\right) + B_{11}\frac{\partial\psi_r}{\partial r} + B_{12}\left(\frac{\psi_r}{r} + \frac{1}{r}\frac{\partial\psi_\theta}{\partial\theta}\right), \\
N_{\theta\theta} &= A_{11}\left(\frac{u_1}{r} + \frac{1}{r}\frac{\partial u_2}{\partial\theta}\right) + A_{12}\frac{\partial u_1}{\partial r} + B_{11}\left(\frac{\psi_r}{r} + \frac{1}{r}\frac{\partial\psi_\theta}{\partial\theta}\right) + B_{12}\frac{\partial\psi_r}{\partial r}, \\
N_{r\theta} &= A_{33}\left(\frac{1}{r}\frac{\partial u_1}{\partial\theta} + \frac{\partial u_2}{\partial r} - \frac{u_2}{r}\right) + B_{33}\left(\frac{1}{r}\frac{\partial\psi_r}{\partial\theta} + \frac{\partial\psi_\theta}{\partial r} - \frac{\psi_\theta}{r}\right), \\
M_{rr} &= B_{11}\frac{\partial u_1}{\partial r} + B_{12}\left(\frac{u_1}{r} + \frac{1}{r}\frac{\partial u_2}{\partial\theta}\right) + D_{11}\frac{\partial\psi_r}{\partial r} + D_{12}\left(\frac{\psi_r}{r} + \frac{1}{r}\frac{\partial\psi_\theta}{\partial\theta}\right), \\
M_{\theta\theta} &= B_{11}\left(\frac{u_1}{r} + \frac{1}{r}\frac{\partial u_2}{\partial\theta}\right) + B_{12}\frac{\partial u}{\partial r} + D_{11}\left(\frac{\psi_r}{r} + \frac{1}{r}\frac{\partial\psi_\theta}{\partial\theta}\right) + D_{12}\frac{\partial\psi_r}{\partial r}, \\
M_{r\theta} &= B_{33}\left(\frac{1}{r}\frac{\partial u_1}{\partial\theta} + \frac{\partial u_2}{\partial r} - \frac{u_2}{r}\right) + D_{33}\left(\frac{1}{r}\frac{\partial\psi_r}{\partial\theta} + \frac{\partial\psi_\theta}{\partial r} - \frac{\psi_\theta}{r}\right), \\
Q_r &= k^2 A_{33}\left(\frac{\partial u_3}{\partial r} + \psi_r\right), \\
Q_\theta &= k^2 A_{33}\left(\frac{1}{r}\frac{\partial u_3}{\partial\theta} + \psi_\theta\right)
\end{aligned} \tag{5}$$

where the parameters A_ξ, B_ξ, $D_\xi (\xi = 11, 12, 33)$ are the material stiffness coefficients of the plate, which can be defined in the following form:

$$(A_\xi, B_\xi, D_\xi) = \int_{-h/2}^{h/2} \left(1, z, z^2\right) Q_\xi \mathrm{d}z. \tag{6}$$

For FG plates with power law function (Eq. (4)), Q_ξ's are defined as

$$\begin{aligned} Q_{11} &= \frac{E_m}{1-\nu^2} + \frac{E_{cm}}{1-\nu^2}\left(\frac{1}{2} - \frac{z}{h}\right)^n, \\ Q_{33} &= \frac{E_m}{2(1+\nu)} + \frac{E_{cm}}{2(1+\nu)}\left(\frac{1}{2} - \frac{z}{h}\right)^n, \\ Q_{12} &= \nu\left(\frac{E_m}{1-\nu^2} + \frac{E_{cm}}{1-\nu^2}\left(\frac{1}{2} - \frac{z}{h}\right)^n\right) \end{aligned} \tag{7}$$

where ν is Poisson's ratio, and due to its small variation, it is assumed to be constant through the thickness. Substituting the resultant forces and moments obtained from Eqs. (5) into (1), the governing equations of motion for an FG annular sector plate are obtained as

$$\begin{aligned} &A_{11}\left(\frac{\partial^2 u_1}{\partial r^2} + \frac{1}{r}\frac{\partial u_1}{\partial r} - \frac{u_1}{r^2} - \frac{1}{r^2}\frac{\partial u_2}{\partial \theta} + \frac{1}{r}\frac{\partial^2 u_2}{\partial r \partial \theta}\right) + A_{33}\left(\frac{1}{r^2}\frac{\partial^2 u_1}{\partial \theta^2} - \frac{1}{r}\frac{\partial^2 u_2}{\partial r \partial \theta} - \frac{1}{r^2}\frac{\partial u_2}{\partial \theta}\right) \\ &\quad + B_{11}\left(\frac{\partial^2 \psi_r}{\partial r^2} + \frac{1}{r}\frac{\partial \psi_r}{\partial r} - \frac{\psi_r}{r^2} - \frac{1}{r^2}\frac{\partial \psi_\theta}{\partial \theta} + \frac{1}{r}\frac{\partial^2 \psi_\theta}{\partial r \partial \theta}\right) + B_{33}\left(\frac{1}{r^2}\frac{\partial^2 \psi_r}{\partial \theta^2} - \frac{1}{r}\frac{\partial^2 \psi_\theta}{\partial r \partial \theta} - \frac{1}{r^2}\frac{\partial \psi_\theta}{\partial \theta}\right) \\ &\quad = I_0 \ddot{u}_1 + I_1 \ddot{\psi}_r, \end{aligned} \tag{8.1}$$

$$\begin{aligned} &A_{11}\left(\frac{1}{r^2}\frac{\partial u_1}{\partial \theta} + \frac{1}{r}\frac{\partial^2 u_1}{\partial r \partial \theta} + \frac{1}{r^2}\frac{\partial^2 u_2}{\partial \theta^2}\right) + A_{33}\left(\frac{-1}{r}\frac{\partial^2 u_1}{\partial r \partial \theta} + \frac{\partial^2 u_2}{\partial r^2} + \frac{1}{r^2}\frac{\partial u_1}{\partial \theta} + \frac{1}{r}\frac{\partial u_2}{\partial r} - \frac{u_2}{r^2}\right) \\ &\quad + B_{11}\left(\frac{1}{r^2}\frac{\partial \psi_r}{\partial \theta} + \frac{1}{r^2}\frac{\partial^2 \psi_\theta}{\partial \theta^2} + \frac{1}{r}\frac{\partial^2 \psi_r}{\partial r \partial \theta}\right) + B_{33}\left(\frac{-1}{r}\frac{\partial^2 \psi_r}{\partial r \partial \theta} + \frac{\partial^2 \psi_\theta}{\partial r^2} + \frac{1}{r^2}\frac{\partial \psi_r}{\partial \theta} + \frac{1}{r}\frac{\partial \psi_\theta}{\partial r} - \frac{\psi_\theta}{r^2}\right) \\ &\quad = I_0 \ddot{u}_2 + I_1 \ddot{\psi}_\theta, \end{aligned} \tag{8.2}$$

$$\begin{aligned} &B_{11}\left(\frac{\partial^2 u_1}{\partial r^2} + \frac{1}{r}\frac{\partial u_1}{\partial r} - \frac{u_1}{r^2} - \frac{1}{r^2}\frac{\partial u_2}{\partial \theta} + \frac{1}{r}\frac{\partial^2 u_2}{\partial r \partial \theta}\right) + B_{33}\left(\frac{1}{r^2}\frac{\partial^2 u_1}{\partial \theta^2} - \frac{1}{r}\frac{\partial^2 u_2}{\partial r \partial \theta} - \frac{1}{r^2}\frac{\partial u_2}{\partial \theta}\right) \\ &\quad + D_{11}\left(\frac{\partial^2 \psi_r}{\partial r^2} + \frac{1}{r}\frac{\partial \psi_r}{\partial r} - \frac{\psi_r}{r^2} - \frac{1}{r^2}\frac{\partial \psi_\theta}{\partial \theta} + \frac{1}{r}\frac{\partial^2 \psi_\theta}{\partial r \partial \theta}\right) + D_{33}\left(\frac{1}{r^2}\frac{\partial^2 \psi_r}{\partial \theta^2} - \frac{1}{r}\frac{\partial^2 \psi_\theta}{\partial r \partial \theta} - \frac{1}{r^2}\frac{\partial \psi_\theta}{\partial \theta}\right) \\ &\quad - k^2 A_{33}\left(\frac{\partial u_3}{\partial r} + \psi_r\right) = I_1 \ddot{u}_1 + I_2 \ddot{\psi}_r, \end{aligned} \tag{8.3}$$

$$\begin{aligned} &B_{11}\left(\frac{1}{r^2}\frac{\partial u_1}{\partial \theta} + \frac{1}{r}\frac{\partial^2 u_1}{\partial r \partial \theta} + \frac{1}{r^2}\frac{\partial^2 u_2}{\partial \theta^2}\right) + B_{33}\left(\frac{-1}{r}\frac{\partial^2 u_1}{\partial r \partial \theta} + \frac{\partial^2 u_2}{\partial r^2} + \frac{1}{r^2}\frac{\partial u_1}{\partial \theta} + \frac{1}{r}\frac{\partial u_2}{\partial r} - \frac{u_2}{r^2}\right) \\ &\quad + D_{11}\left(\frac{1}{r^2}\frac{\partial \psi_r}{\partial \theta} + \frac{1}{r^2}\frac{\partial^2 \psi_\theta}{\partial \theta^2} + \frac{1}{r}\frac{\partial^2 \psi_r}{\partial r \partial \theta}\right) + D_{33}\left(\frac{-1}{r}\frac{\partial^2 \psi_r}{\partial r \partial \theta} + \frac{\partial^2 \psi_\theta}{\partial r^2} + \frac{1}{r^2}\frac{\partial \psi_r}{\partial \theta} + \frac{1}{r}\frac{\partial \psi_\theta}{\partial r} - \frac{\psi_\theta}{r^2}\right) \\ &\quad - k^2 A_{33}\left(\frac{1}{r}\frac{\partial u_3}{\partial \theta} + \psi_\theta\right) = I_1 \ddot{u}_2 + I_2 \ddot{\psi}_\theta, \end{aligned} \tag{8.4}$$

$$k^2 A_{33}\left(\frac{\partial^2 u_3}{\partial r^2} + \frac{1}{r}\frac{\partial u_3}{\partial r} + \frac{1}{r^2}\frac{\partial^2 u_3}{\partial \theta^2} + \frac{\partial \psi_r}{\partial r} + \frac{1}{r}\frac{\partial \psi_\theta}{\partial \theta} + \frac{\psi_r}{r}\right) = I_0 . \ddot{u}_3. \tag{8.5}$$

Equations (8) are five highly coupled partial differential equations in terms of in-plane displacements, rotation functions, and transverse displacements. For solving these equations analytically, it is desirable to find a method for decoupling them [29,30]. Using the following analytical method, these governing equations will be decoupled.

Equation (8) can be easily rewritten in the following form:

$$A_{11}\frac{\partial\varphi_1}{\partial r}+A_{33}\frac{1}{r}\frac{\partial\varphi_2}{\partial\theta}+B_{11}\frac{\partial\varphi_3}{\partial r}+B_{33}\frac{1}{r}\frac{\partial\varphi_4}{\partial\theta}=I_0\ddot{u}_1+I_1\ddot{\psi}_r, \tag{9.1}$$

$$A_{11}\frac{1}{r}\frac{\partial\varphi_1}{\partial\theta}-A_{33}\frac{\partial\varphi_2}{\partial r}+B_{11}\frac{1}{r}\frac{\partial\varphi_3}{\partial\theta}-B_{33}\frac{\partial\varphi_4}{\partial r}=I_0\ddot{u}_2+I_1\ddot{\psi}_\theta, \tag{9.2}$$

$$B_{11}\frac{\partial\varphi_1}{\partial r}+B_{33}\frac{1}{r}\frac{\partial\varphi_2}{\partial\theta}+D_{11}\frac{\partial\varphi_3}{\partial r}+D_{33}\frac{1}{r}\frac{\partial\varphi_4}{\partial\theta}-k^2A_{33}\left(\frac{\partial u_3}{\partial r}+\psi_r\right)=I_1\ddot{u}_1+I_2\ddot{\psi}_r, \tag{9.3}$$

$$A_{11}\frac{1}{r}\frac{\partial\varphi_1}{\partial\theta}-A_{33}\frac{\partial\varphi_2}{\partial r}+B_{11}\frac{1}{r}\frac{\partial\varphi_3}{\partial\theta}-B_{33}\frac{\partial\varphi_4}{\partial r}-k^2A_{33}\left(\frac{1}{r}\frac{\partial u_3}{\partial\theta}+\psi_\theta\right)=I_1\ddot{u}_2+I_2\ddot{\psi}_\theta, \tag{9.4}$$

$$k^2A_{33}\left(\nabla^2u_3+\varphi_3\right)=I_0\ddot{u}_3 \tag{9.5}$$

where ∇^2 is the Laplace operator in polar coordinates $\left(\nabla^2=\frac{\partial^2}{\partial r^2}+\frac{1}{r}\frac{\partial}{\partial r}+\frac{1}{r^2}\frac{\partial^2}{\partial\theta^2}\right)$, and the variables φ_1, φ_2, φ_3 and φ_4 are defined as

$$\begin{aligned}
\varphi_1&=\frac{\partial u_1}{\partial r}+\frac{u_1}{r}+\frac{1}{r}\frac{\partial u_2}{\partial\theta},\\
\varphi_2&=\frac{1}{r}\frac{\partial u_1}{\partial\theta}-\frac{\partial u_2}{\partial r}-\frac{u_2}{r},\\
\varphi_3&=\frac{\partial\psi_r}{\partial r}+\frac{\psi_r}{r}+\frac{1}{r}\frac{\partial\psi_\theta}{\partial\theta},\\
\varphi_4&=\frac{1}{r}\frac{\partial\psi_r}{\partial\theta}-\frac{\partial\psi_\theta}{\partial r}-\frac{\psi_\theta}{r}.
\end{aligned} \tag{10}$$

Also, Eqs. (9.1) and (9.2) can be rewritten in the following form:

$$\begin{aligned}
B_{11}\frac{\partial\varphi_1}{\partial r}+B_{33}\frac{1}{r}\frac{\partial\varphi_2}{\partial\theta}&=-\frac{B_{11}^2}{A_{11}}\frac{\partial\varphi_3}{\partial r}-\frac{B_{33}B_{11}}{A_{11}}\frac{1}{r}\frac{\partial\varphi_4}{\partial\theta}+\frac{B_{11}}{A_{11}}I_0\ddot{u}_1+\frac{B_{11}}{A_{11}}I_1\ddot{\psi}_r,\\
B_{11}\frac{1}{r}\frac{\partial\varphi_1}{\partial\theta}-B_{33}\frac{\partial\varphi_2}{\partial r}&=-\frac{B_{11}^2}{A_{11}}\frac{1}{r}\frac{\partial\varphi_3}{\partial\theta}+\frac{B_{33}B_{11}}{A_{11}}\frac{\partial\varphi_4}{\partial r}+\frac{B_{11}}{A_{11}}I_0\ddot{u}_2+\frac{B_{11}}{A_{11}}I_1\ddot{\psi}_\theta.
\end{aligned} \tag{11}$$

Substituting Eqs. (11) into (9.3) and (9.4) yields

$$\begin{aligned}
&\left(D_{11}-\frac{B_{11}^2}{A_{11}}\right)\frac{\partial\varphi_3}{\partial r}+\left(D_{33}-\frac{B_{33}B_{11}}{A_{11}}\right)\left(\frac{1}{r}\frac{\partial\varphi_4}{\partial\theta}\right)-k^2A_{33}\left(\frac{\partial u_3}{\partial r}+\psi_r\right)\\
&\quad=\left(I_1-\frac{B_{11}}{A_{11}}I_0\right)\ddot{u}_1+\left(I_2-\frac{B_{11}}{A_{11}}I_1\right)\ddot{\psi}_r,
\end{aligned} \tag{12.1}$$

$$\begin{aligned}
&\left(D_{11}-\frac{B_{11}^2}{A_{11}}\right)\left(\frac{1}{r}\frac{\partial\varphi_3}{\partial\theta}\right)-\left(D_{33}-\frac{B_{33}B_{11}}{A_{11}}\right)\frac{\partial\varphi_4}{\partial r}-k^2A_{33}\left(\frac{1}{r}\frac{\partial u_3}{\partial\theta}+\psi_\theta\right)\\
&\quad=\left(I_1-\frac{B_{11}}{A_{11}}I_0\right)\ddot{u}_2+\left(I_2-\frac{B_{11}}{A_{11}}I_1\right)\ddot{\psi}_\theta.
\end{aligned} \tag{12.2}$$

By differentiating Eqs. (12.1) and (12.2) with respect to r and θ, respectively, and doing some algebraic operations, the following partial differential equations are obtained:

$$\hat{D}\nabla^2\varphi_3-k^2A_{33}\left(\nabla^2u_3+\varphi_3\right)=J_1\ddot{\varphi}_1+J_2\ddot{\varphi}_3, \tag{13.1}$$

$$\hat{C}\nabla^2\varphi_4-k^2A_{33}\varphi_4=J_1\ddot{\varphi}_2+J_2\ddot{\varphi}_4 \tag{13.2}$$

where

$$\hat{D} = D_{11} - \frac{B_{11}^2}{A_{11}}, \quad \hat{C} = D_{33} - \frac{B_{11}B_{33}}{A_{11}},$$
$$J_1 = I_1 - \frac{B_{11}}{A_{11}}I_0, \quad J_2 = I_2 - \frac{B_{11}}{A_{11}}I_1. \tag{14}$$

Similarly, differentiating Eqs. (9.1) and (9.2) with respect to r and θ, respectively, and doing some algebraic calculations, gives the following relations:

$$A_{11}\nabla^2\varphi_1 + B_{11}\nabla^2\varphi_3 = I_0\ddot{\varphi}_1 + I_1\ddot{\varphi}_3, \tag{15.1}$$
$$A_{33}\nabla^2\varphi_2 + B_{33}\nabla^2\varphi_4 = I_0\ddot{\varphi}_2 + I_1\ddot{\varphi}_4 \tag{15.2}$$

calculating the parameter φ_3 from Eq. (9.5) and replacing it into Eq. (15.1), the parameter φ_1 can be obtained in terms of the transverse displacement u_3. Introducing the results into Eq. (13.1) yields

$$\nabla^6 u_3 + \kappa_1\nabla^4\ddot{u}_3 + \kappa_2\nabla^2\ddot{u}_3 + \kappa_3\nabla^2\ddot{\ddot{u}}_3 + \kappa_4\ddot{\ddot{u}}_3 + \kappa_5\ddot{\ddot{\ddot{u}}}_3 = 0. \tag{16}$$

Also, by considering Eq. (13.2), the parameter φ_2 can be obtained in terms of the parameter φ_4. Then, by substituting the result into Eq. (15.2), it can be concluded that

$$\nabla^4\varphi_4 + \kappa_6\nabla^2\varphi_4 + \kappa_7\nabla^2\ddot{\varphi}_4 + \kappa_8\ddot{\varphi}_4 + \kappa_9\ddot{\ddot{\varphi}}_4 = 0 \tag{17}$$

where the parameters $\kappa_j \quad (j = 1, \ldots, 9)$ are defined as

$$\kappa_1 = \frac{I_0}{A_{11}} + \frac{I_0}{k^2A_{33}} + \frac{J_2}{\hat{D}} - \frac{B_{11}J_1}{\hat{D}A_{11}}, \quad \kappa_2 = -\frac{I_0}{\hat{D}},$$
$$\kappa_3 = \frac{I_0J_2}{k^2A_{33}\hat{D}} - \frac{I_0B_{11}J_1}{k^2A_{33}\hat{D}A_{11}} + \frac{I_0^2}{k^2A_{33}A_{11}} + \frac{I_0J_2}{\hat{D}A_{11}} - \frac{I_1J_1}{\hat{D}A_{11}}, \quad \kappa_4 = -\frac{I_0^2}{\hat{D}A_{11}},$$
$$\kappa_5 = \frac{I_0^2J_2}{k^2A_{33}\hat{D}A_{11}} - \frac{I_0I_1J_1}{k^2A_{33}\hat{D}A_{11}}, \quad \kappa_6 = -\frac{k^2A_{33}}{\hat{C}}, \quad \kappa_7 = -\frac{B_{33}J_1}{\hat{C}A_{33}} + \frac{J_2}{\hat{C}} + \frac{I_0}{A_{33}},$$
$$\kappa_8 = -\frac{k^2I_0}{\hat{C}}, \quad \kappa_9 = -\frac{I_1J_1}{\hat{C}A_{33}} + \frac{I_0J_2}{\hat{C}A_{33}}. \tag{18}$$

Therefore, the five coupled partial differential Eq. (8) have been converted into two decoupled Eqs. (16) and (17), which are in terms of the transverse displacement u_3 and the new function φ_4. Using these decoupled equations, the free vibration analysis of FG annular sector plates can be analytically investigated.

It is noted that in the special case of static loading a similar method has been previously investigated for decoupling the governing equations of equilibrium for functionally graded circular plates by Nosier and Fallah [30]. Moreover, another method has been performed for decoupling the governing equations of plates by assigning a different plane from $z = 0$ (see Irschik [31] and Naderi and Saidi [32]).

3 Solution

It is assumed that the annular sector plate has simply supported boundary conditions in radial edges and arbitrary boundary conditions at the circular edges. The boundary conditions of simply supported radial edges can be written as

$$u_3(r,\theta) = M_{\theta\theta}(r,\theta) = \psi_r(r,\theta) = N_{\theta\theta}(r,\theta) = u(r,\theta) = 0 \quad \text{at } \theta = 0, \beta. \tag{19}$$

In order to satisfy the conditions (19), the displacement components and rotation functions are expressed as

$$\begin{aligned}
u_3 &= \sum_{m=1}^{\infty} u_{3m}(r)\sin(\mu_m\theta)\; e^{i\omega_m t},\\
u_1 &= \sum_{m=1}^{\infty} u_{1m}(r)\sin(\mu_m\theta)\; e^{i\omega_m t},\\
u_2 &= \sum_{m=1}^{\infty} u_{2m}(r)\cos(\mu_m\theta)\; e^{i\omega_m t},\\
\psi_r &= \sum_{m=1}^{\infty} \psi_{rm}(r)\sin(\mu_m\theta)\; e^{i\omega_m t},\\
\psi_\theta &= \sum_{m=1}^{\infty} \psi_{\theta m}(r)\cos(\mu_m\theta)\; e^{i\omega_m t}
\end{aligned} \tag{20}$$

where $\mu_m = (m\pi/\beta)$ and ω_m is the natural frequency. Also, by the help of Eq. (10), the parameter φ_4 can be obtained as

$$\varphi_4 = \sum_{m=1}^{\infty} \varphi_m(r)\cos(\mu_m\theta)\; e^{i\omega_m t}. \tag{21}$$

By substituting Eqs. (20) and (21) into (16) and (17), two ordinary differential equations are obtained as

$$\begin{gathered}
\frac{\mathrm{d}^6 u_{3m}}{\mathrm{d}r^6} + \frac{3}{r}\frac{\mathrm{d}^5 u_{3m}}{\mathrm{d}r^5} + \eta_1\frac{\mathrm{d}^4 u_{3m}}{\mathrm{d}r^4} + \eta_2\frac{\mathrm{d}^3 u_{3m}}{\mathrm{d}r^3} + \eta_3\frac{\mathrm{d}^2 u_{3m}}{\mathrm{d}r^2} + \eta_4\frac{\mathrm{d}u_{3m}}{\mathrm{d}r} + \eta_5 u_{3m}(r) = 0,\\
\frac{\mathrm{d}^4\varphi_m}{\mathrm{d}r^4} + \frac{2}{r}\frac{\mathrm{d}^3\varphi_m}{\mathrm{d}r^3} + \eta_6\frac{\mathrm{d}^2\varphi_m}{\mathrm{d}r^2} + \eta_7\frac{\mathrm{d}\varphi_m}{\mathrm{d}r} + \eta_8\varphi_m(r) = 0
\end{gathered} \tag{22}$$

where

$$\begin{aligned}
\eta_1 &= -\left(\kappa_1\omega_m^2 + \frac{3}{r^2} + \frac{3\mu_m^2}{r^2}\right),\\
\eta_2 &= \left(\frac{6\mu_m^2}{r^3} + \frac{6}{r^3} - \frac{2\kappa_1\omega_m^2}{r}\right),\\
\eta_3 &= \left(\kappa_3\omega_m^4 - \kappa_2\omega_m^2 - \frac{9}{r^4} + \frac{\kappa_1\omega_m^2}{r^2} - \frac{21\mu_m^2}{r^4} + \frac{3\mu_m^4}{r^4} + \frac{2\kappa_1\omega_m^2\mu_m^2}{r^2}\right),\\
\eta_4 &= \left(\frac{45\mu_m^2}{r^5} + \frac{\kappa_3\omega_m^4}{r} - \frac{9\mu_m^4}{r^5} + \frac{9}{r^5} - \frac{\kappa_2\omega_m^2}{r} - \frac{2\kappa_1\omega_m^2\mu_m^2}{r^3} - \frac{\kappa_1\omega_m^2}{r^3}\right),\\
\eta_5 &= \left(\frac{\kappa_2\omega_m^2\mu_m^2}{r^2} - \frac{64\mu_m^2}{r^6} - \kappa_6\omega_m^6 + \frac{20\mu_m^4}{r^6} + \frac{4\kappa_1\omega_m^2\mu_m^2}{r^4} - \frac{\kappa_1\omega_m^2\mu_m^4}{r^4} - \frac{\kappa_3\omega_m^4\mu_m^2}{r^2} - \frac{\mu_m^6}{r^6} + \kappa_4\omega^4\right),\\
\eta_6 &= \left(\kappa_6 + \kappa_7 - \frac{1+2\mu_m^2}{r^2}\right),\\
\eta_7 &= \left(\frac{1+2\mu_m^2}{r^3} + \frac{\kappa_6+\kappa_7}{r}\right),\\
\eta_8 &= \left(\kappa_9\omega_m^4 - \kappa_8\omega_m^2 - \frac{\kappa_7\mu_m^2}{r^2} - \frac{\kappa_6\mu_m^2}{r^2} + \frac{\mu_m^4}{r^4} - \frac{4\mu_m^2}{r^4}\right).
\end{aligned} \tag{23}$$

Equations (22) are two ordinary differential equations in terms of u_{3m} and φ_m. The solutions of these differential equations are obtained as

$$
\begin{aligned}
u_{3m}(r) &= C_1 I_{\mu_m}\left(\sqrt{\lambda_1} r\right) + C_2 K_{\mu_m}\left(\sqrt{\lambda_1} r\right) + C_3 J_{\mu_m}\left(\sqrt{\lambda_2} r\right) + C_4 Y_{\mu_m}\left(\sqrt{\lambda_2} r\right) \\
&\quad + C_5 J_{\mu_m}\left(\sqrt{\lambda_3} r\right) + C_6 Y_{\mu_m}\left(\sqrt{\lambda_3} r\right), \\
\varphi_m(r) &= C_7 J_{\mu_m}(\lambda_4 r) + C_8 Y_{\mu_m}(\lambda_4 r) + C_9 I_{\mu_m}(\lambda_5 r) + C_{10} K_{\mu_m}(\lambda_5 r),
\end{aligned} \tag{24}
$$

where J and Y are the Bessel functions of the first and second kinds. Also, I and K are the modified Bessel functions of the first and second kinds, and $C_k (k = 1, \ldots, 10)$ are the integration constants. The parameters $\lambda_k (k = 1, \ldots, 5)$ in Eq. (24) are as follows:

$$
\begin{aligned}
\lambda_1 &= \frac{1}{6}\left(-\frac{T}{\gamma_1} + \frac{4\left(3\gamma_3\gamma_1 - \gamma_2^2\right)}{\gamma_1 T} - \frac{2\gamma_2}{\gamma_1}\right), \\
\lambda_2 &= \frac{1}{12}\left(-\frac{T}{\gamma_1} + \frac{4\left(3\gamma_3\gamma_1 - \gamma_2^2\right)}{\gamma_1 T} - \frac{4\gamma_2}{\gamma_1} + 6\sqrt{3}i\left(\frac{T}{6\gamma_1} + \frac{2}{3}\frac{3\gamma_3\gamma_1 - \gamma_2^2}{\gamma_1 T}\right)\right), \\
\lambda_3 &= \frac{1}{12}\left(\frac{T}{\gamma_1} - \frac{4\left(3\gamma_3\gamma_1 - \gamma_2^2\right)}{\gamma_1 T} + \frac{4\gamma_2}{\gamma_1} + 6\sqrt{3}i\left(\frac{T}{6\gamma_1} + \frac{2}{3}\frac{3\gamma_3\gamma_1 - \gamma_2^2}{\gamma_1 T}\right)\right), \\
\lambda_4 &= \frac{\sqrt{2}}{2}\left(\sqrt{\frac{\gamma_6 - \sqrt{\gamma_6^2 - 4\gamma_5\gamma_7}}{\gamma_5}}\right), \\
\lambda_5 &= \frac{\sqrt{2}}{2}\left(\sqrt{\frac{\gamma_6 + \sqrt{\gamma_6^2 - 4\gamma_5\gamma_7}}{\gamma_5}}\right).
\end{aligned} \tag{25}
$$

In the above equations, $i = \sqrt{-1}$ and the parameters $\gamma_k (k = 1, \ldots, 7)$ and T are defined as

$$
\begin{aligned}
\gamma_1 &= \frac{\hat{D} A_{11}}{J_1 \omega_m^2}, \\
\gamma_2 &= \left(\frac{\hat{D} I_0}{k^2 A_{33} J_1} + \frac{J_2}{J_1}\right) A_{11} - B_{11} + \frac{\hat{D} I_0}{J_1}, \\
\gamma_3 &= -\left(\frac{I_0}{J_1} - \frac{I_0 J_2 \omega_m^2}{k^2 A_{33} J_1}\right) A_{11} - \frac{I_0 B_{11} \omega_m^2}{k^2 A_{33}} + I_0 \omega_m^2 \left(\frac{\hat{D} I_0}{k^2 A_{33} J_1} + \frac{J_2}{J_1}\right) - I_1 \omega_m^2, \\
\gamma_4 &= -\left(\frac{I_0}{J_1} - \frac{I_0 J_2 \omega_m^2}{k^2 A_{33} J_1}\right) I_0 \omega_m^2 - \frac{I_0 I_1 \omega_m^4}{k^2 A_{33}}, \\
\gamma_5 &= -\frac{\hat{C} A_{33}}{J_1 \omega_m^2}, \\
\gamma_6 &= \frac{k^2 A_{33}^2}{J_1 \omega_m^2} - \frac{J_2 A_{33}}{J_1} + B_{33} - \frac{\hat{C} I_0}{J_1}, \\
\gamma_7 &= \frac{k^2 A_{33} I_0}{J_1} - \frac{J_2 I_0 \omega_m^2}{J_1} + I_1 \omega_m^2.
\end{aligned} \tag{26}
$$

$$
T = \left(36\gamma_1\gamma_3\gamma_2 - 108\gamma_4\gamma_1^2 - 8\gamma_2^3 + 12\sqrt{3}\gamma_1\sqrt{4\gamma_1\gamma_3^3 - \gamma_3^2\gamma_2^2 - 18\gamma_1\gamma_3\gamma_2\gamma_4 + 27\gamma_3^2\gamma_1^2 + 4\gamma_3\gamma_2^3}\right)^{\frac{1}{3}}.
$$

Table 1 Comparison of the natural frequency of the annular sector plate, $\varpi = \omega b^2\sqrt{\frac{\rho h}{D}}$, for all boundary conditions ($h/b = 0.1$, $\beta = 210°$)

		$a/b = 0.1$	$a/b = 0.3$	$a/b = 0.5$	$a/b = 0.7$
SSCC	Ref. [8]	25.4720	40.0983	70.7344	152.400
	Present	25.47196	40.09826	70.73435	152.40023
SSCS	Ref. [8]	17.4921	28.2618	51.8931	120.446
	Present	17.49211	28.26181	51.89315	120.44582
SSCF	Ref. [8]	3.3866	6.3364	12.6589	34.0826
	Present	3.386564	6.33636	12.65894	34.08261
SSSC	Ref. [8]	22.8396	32.3481	55.9461	125.435
	Present	22.83959	32.34811	55.94611	125.43512
SSSS	Ref. [8]	15.4157	21.7428	38.4554	94.006
	Present	15.41571	21.74284	38.45537	43.93197 − 94.00594
SSSF	Ref. [8]	2.4835	3.2811	4.5837	7.5976
	Present	2.48354	3.28106	4.58370	7.59760
SSFC	Ref. [8]	18.6816	16.6137	19.6097	40.4640
	Present	18.68161	16.61369	19.60973	40.46403
SSFS	Ref. [8]	12.3566	10.7753	9.6643	11.0879
	Present	12.35664	10.77533	9.66428	11.08787
SSFF	Ref. [8]	0.5952	0.4126	0.3113	0.2388
	Present	0.59516	0.412575	0.31129	0.23877

The parameters $\varphi_{km}(k = 1, \ldots, 3)$, ψ_{rm}, $\psi_{\theta m}$, u_{1m} and u_{2m} are shown in the Appendix in terms of Bessel functions.

In order to obtain the natural frequencies of FG annular sector plates, the corresponding boundary conditions at circular edges should be satisfied.

4 Boundary conditions

The natural frequencies of the FG annular sector plate can be obtained by imposing the arbitrary boundary conditions at two circular edges. Depending on specific boundary conditions, each of the edges has one of the following conditions:

$$\text{Clamped:} \quad u_1(r,\theta) = u_2(r,\theta) = u_3(r,\theta) = \psi_r(r,\theta) = \psi_\theta(r,\theta) = 0 \quad \text{at } r = a, b, \tag{27.1}$$

$$\text{Simply supported:} \; u_3(r,\theta) = M_{rr}(r,\theta) = N_{rr}(r,\theta) = u_2(r,\theta)) = \psi_\theta(r,\theta) = 0 \quad \text{at } r = a, b, \tag{27.2}$$

$$\text{Free:} \quad N_{rr}(r,\theta) = N_{r\theta}(r,\theta) = M_{rr}(r,\theta) = M_{r\theta}(r,\theta) = Q_r(r,\theta) = 0 \quad \text{at } r = a, b. \tag{27.3}$$

By imposing arbitrary boundary conditions along the circular edges at $r = a$ and $r = b$, ten homogeneous algebraic equations are obtained. Setting the characteristic determinant of the tenth-order coefficient matrix equal to zero, the natural frequencies of the FG annular sector plate can be evaluated. The FG annular sector plates have simply supported radial edges and arbitrary boundary conditions along the circular edges which are identified according to the inner and outer radius boundary conditions (e.g. *SSCF* denotes an annular sector plate with simply supported radial edges, clamped inner and free outer circular edges). The nine possible boundary conditions containing *SSSS, SSCC, SSFF, SSCF, SSFC, SSCS, SSSC, SSSF*, and *SSFS* are considered for presenting the numerical results.

5 Validation

To validate the accuracy of the formulations, the comparison studies of the results are carried out with those available in the literature.

In Table 1, for the special case of $n = 0$, the frequencies of a homogeneous annular sector plate with various boundary conditions are compared with those reported by Ref. [8], and a good agreement can be seen. It is noticeable that for *SSSS* boundary conditions and $a/b = 0.7$, the corresponding frequency reported by Ref. [8] is the second frequency, and for this reason, both frequencies are presented.

Nie and Zhong [25] presented a vibration analysis of FG annular sectorial plates with simply supported radial edges using differential quadrature method (DQM). They considered that the material properties vary

Table 2 Comparison of the non-dimensional frequency of *SSCC* annular sector FG plate $\left(\Omega = \omega h \sqrt{(1+\nu)(1-2\nu)\rho_c/E_c(1-\nu)}\right)$

β (deg)	a/b		$n=1$	$n=2$	$n=3$	$n=4$	$n=5$
195	0.1	Ref. [25]	0.0663	0.0622	0.0566	0.0505	0.0446
		Present	0.0664	0.0625	0.0571	0.0510	0.0451
	0.3	Ref. [25]	0.1041	0.0980	0.0895	0.0801	0.0710
		Present	0.1046	0.0989	0.0908	0.0815	0.0723
210	0.1	Ref. [25]	0.0659	0.0619	0.0563	0.0502	0.0443
		Present	0.0659	0.0620	0.0566	0.0506	0.0447
	0.3	Ref. [25]	0.1039	0.0978	0.0892	0.0799	0.0708
		Present	0.1043	0.0986	0.0905	0.0812	0.0720

exponentially along the thickness. In order to compare the results with those presented in Ref. [25], it is assumed that the material properties vary exponentially along the thickness in the present formulation. The material coefficients have been obtained based on the exponential model, and the non-dimensional frequencies have been compared in Table 2 with those presented in Ref. [25]. It can be seen that the results are close to each other.

6 Numerical results and discussions

For numerical results, a functionally graded material composed of aluminum (as metal) and alumina (as ceramic) is considered. Young's modulus and density of aluminum are $E_m = 70\,\text{GPa}$, $\rho_m = 2{,}707\,\text{Kg/m}^3$ and for alumina $E_c = 380\,\text{GPa}$, $\rho_c = 3{,}800\,\text{Kg/m}^3$. The Poisson's ratio of the plate is assumed to be constant through the thickness and equal to 0.3.

For generalization, the following non-dimensional natural frequency is used for numerical results:

$$\varpi = \omega b^2 \sqrt{\frac{\rho_m h}{D_m}} \tag{4}$$

where D_m is the flexural rigidity of the full-metal plate, i.e.

$$D_m = \frac{E_m h^3}{12(1-\nu^2)}. \tag{5}$$

The first three non-dimensional frequencies are shown for all possible nine boundary conditions along the circular edges in Tables 3, 4, 5, 6, 7, 8, 9, 10, and 11 for different powers of FGM, aspect ratios 0.5 and 0.7, and thickness/length ratio h/c, $(c = b - a)$, 0.1 and 0.2 for over a range of sector angles. In these Tables, the numbers in parentheses present the wave numbers in the r and θ directions, respectively.

It can be seen that for all boundary conditions the value of the natural frequency decreases by increasing the sector angle. Also, by increasing the power law index, the value of frequency decreases.

It can be also seen that the variations of the thickness, aspect ratio, sector angle, and boundary condition of the FG annular sector plates can change the wave number. For example, the results in Table 4 for *SSSS* FG annular sector plates, by increasing the sector angle for $a/b = 0.5$ from $\beta = 45°$ to $\beta = 120°$, the number of waves in the third mode of vibration changes from (1, 3) to (3, 1). Also, by increasing the thickness/length ratio, the non-dimensional frequency decreases, while the value of the natural frequency increases.

In Table 11, the variation of the wave number is significant for an *SSFF* FG annular sector plate with $\beta = 360°$. The value of frequency of mode (3, 1) is lower than that of mode (1, 2). The reason is that the variation of the wave number is more convenient in r direction than θ direction when the circular edges are free.

Figure 2 shows the variation of the fundamental frequency versus the variation of the aspect ratio for all possible boundary conditions. This figure indicates that the value of the fundamental frequency decreases by increasing the aspect ratio up to a point and then it starts increasing by further increase in aspect ratio except for *SSFS, SSFF*, and *SSSF* boundary conditions where the fundamental frequency decreases by increasing the aspect ratio. For an FG annular sector plate with one free edge, the natural frequency decreases with increasing the aspect ratio for small aspect ratios. In fact by increasing the aspect ratio, the length of the free edge increases, and

Table 3 Frequency parameters, $\varpi = \omega b^2 \sqrt{\frac{\rho_m h}{D_m}}$, of *SSCC* FG annular sector plate for third mode sequence number and for some values of n, β, h/c, and a/b

β (deg)	h/c	a/b	$n = 0$	$n = 0.5$	$n = 1$	$n = 2$
45	0.1	0.5	194.9900(1,1)	166.3153(1,1)	150.2992(1,1)	136.4535(1, 1)
			318.6768(2,1)	271.9694(2,1)	245.7534(2,1)	222.9487(2, 1)
			523.8126(3,1)	448.1342(3,1)	405.2020(3,1)	367.2070(3, 1)
		0.7	476.6814(1,1)	406.4655(1,1)	367.3109(1,1)	333.5481(1, 1)
			554.5599(2,1)	473.0050(2,1)	427.4472(2,1)	388.0598(2, 1)
			708.4884(3,1)	604.4198(3,1)	546.15909(3,1)	495.6549(3, 1)
	0.2	0.5	163.6200(1,1)	141.2456(1,1)	128.2741(1,1)	116.1744(1, 1)
			262.0207(2,1)	226.2043(2,1)	205.2594(2,1)	185.6087(2, 1)
			399.3279 (1,3)	353.3567(3,1)	321.0431(3,1)	289.8407(3, 1)
		0.7	402.0732(1,1)	347.2862(1,1)	315.5654(1,1)	285.9592(1, 1)
			464.9412(2,1)	401.3749(2,1)	364.5042(2,1)	330.0968(2, 1)
			589.9567(3,1)	508.9939(3,1)	461.9006(3,1)	417.9694(3, 1)
120	0.1	0.5	167.0994(1,1)	142.4833(1,1)	128.7597(1,1)	116.9292(1, 1)
			179.8915(2,1)	153.4234(2,1)	138.6513(2,1)	125.8944(2, 1)
			204.8409(3,1)	174.7218(3,1)	157.8926(3,1)	143.3371(3, 1)
		0.7	457.7902(1,1)	390.2906(1,1)	352.6789(1,1)	320.2881(1, 1)
			466.8329(2,1)	398.0363(2,1)	359.6869(2,1)	326.6385(2, 1)
			482.8801(3,1)	411.7683(3,1)	372.1060(3,1)	337.8942(3, 1)
	0.2	0.5	141.0583(1,1)	121.8502(1,1)	110.7335(1,1)	100.3574(1, 1)
			151.2281(2,1)	130.6040(2,1)	118.6534(2,1)	107.4946(2, 1)
			171.7523(3,1)	148.2305(3,1)	134.5894(3,1)	121.8738(3, 1)
		0.7	387.5902(1,1)	334.7615(1,1)	304.2132(1,1)	275.7413(1, 1)
			394.4463(2,1)	340.6977(2,1)	309.5957(2.1)	280.5835(2, 1)
			406.9396(3,1)	351.4840(3,1)	319.3671(3,1)	289.3846(3, 1)
240	0.1	0.5	164.2395(1,1)	140.0329(1,1)	126.5425(1,1)	114.9202(1, 1)
			167.0994(2,1)	142.4833(2,1)	128.7598(2,1)	116.9292(2, 1)
			172.1827(3,1)	146.8338(3,1)	132.6946(3,1)	120.4951(3, 1)
		0.7	455.6029(1,1)	388.4161(1,1)	350.9826(1,1)	318.7510(1, 1)
			457.7901(2,1)	390.2906(2,1)	352.6789(2,1)	320.2880(2, 1)
			461.5017(3,1)	393.4705(3,1)	355.5562(3,1)	322.8954(3, 1)
	0.2	0.5	138.8856(1,1)	119.9719(1,1)	109.0317(1,1)	98.8268(1, 1)
			141.0583(2,1)	121.8501(2,1)	110.7335(2,1)	100.3574(2, 1)
			145.0322(3,1)	125.2760(3,1)	113.8345(3,1)	103.1502(3, 1)
		0.7	385.9583(1,1)	333.3460(1,1)	302.9291(1,1)	274.5871(1, 1)
			387.5902(2,1)	334.7615(2,1)	304.2131(2,1)	275.7412(2, 1)
			390.3844(3,1)	337.1827(3,1)	306.4091(3,1)	277.7160(3, 1)
360	0.1	0.5	163.7265(1,1)	139.5932(1,1)	126.1445(1,1)	114.5596(1, 1)
			164.9665(2,1)	140.6560(2,1)	127.1064(2,1)	115.4312(2, 1)
			167.0994(3,1)	142.4833(3,1)	128.7598(3,1)	116.9292(3, 1)
		0.7	455.2013(1,1)	388.0718(1,1)	350.6709(1,1)	318.4687(1, 1)
			456.1671(2,1)	388.8996(2,1)	351.4202(2,1)	319.1475(2, 1)
			457.7902(3,1)	390.2906(3,1)	352.6789(3,1)	320.2881(3, 1)
	0.2	0.5	138.5023(1,1)	119.6398(1,1)	108.7308(1,1)	98.5563(1, 1)
			139.4325(2,1)	120.4451(2,1)	109.4607(2,1)	99.2124(2, 1)
			141.0583(3,1)	121.8502(3,1)	110.7335(3,1)	100.3575(3, 1)
		0.7	385.6598(1,1)	333.0870(1,1)	302.6941(1,1)	274.3758(1, 1)
			386.3781(2,1)	333.7103(2,1)	303.2595(2,1)	274.8840(2, 1)
			387.5902(3,1)	334.7615(3,1)	304.2132(3,1)	275.7413(3, 1)

it causes to decrease the stiffness of the annular sector plate. However, for *SSCF* and *SSFC* annular sector plates, the natural frequency will increase with increasing the aspect ratio for higher values of the aspect ratio. Also, it can be concluded that the effect of the outer edge boundary condition on the natural frequency is significant for $a/b < 0.2$.

Figure 3 shows the variation of the fundamental frequency versus the variation of the sector angle for all nine boundary conditions. It can be seen that for $\beta < 60°$, with increasing the sector angle, the fundamental natural frequency decreases rapidly, whereas the variation of the fundamental frequency is very small for $\beta > 60°$. However, for annular sector plates with *SSCF* boundary condition, the value of the fundamental frequency decreases in the first part and then increases with increasing the sector angle. It can be also seen that

Table 4 Frequency parameters, $\varpi = \omega b^2\sqrt{\frac{\rho_m h}{D_m}}$, of an *SSSS* FG annular sector plate for the third mode sequence number and for some values of n, β, h/c, and a/b

β (deg)	h/c	a/b	$n=0$	$n=0.5$	$n=1$	$n=2$
45	0.1	0.5	130.3982(1, 1)	110.6831(1, 1)	99.8062(1, 1)	90.6573(1, 1)
			278.3881(2, 1)	236.8862(2, 1)	213.7638(2, 1)	193.9860(2, 1)
			391.7539(1, 3)	351.5134(1, 3)	325.6960(1, 3)	294.1509(1, 3)
		0.7	254.3541(1, 1)	215.7466(1, 1)	194.5049(1, 1)	176.7227(1, 1)
			378.2454(2, 1)	321.0869(2, 1)	289.5403(2, 1)	262.9895(2, 1)
			578.4317(3, 1)	491.6330(3, 1)	443.4933(3, 1)	402.6358(3, 1)
	0.2	0.5	120.4116(1, 1)	102.7887(1, 1)	92.8479(1, 1)	84.1620(1, 1)
			195.8769(1, 2)	175.7030(1, 2)	162.7169(1, 2)	146.8519(1, 2)
			289.6496(1, 3)	249.3676(1, 3)	225.8955(1, 3)	204.2066(1, 3)
		0.7	239.9282(1, 1)	204.3913(1, 1)	184.5069(1, 1)	167.3706(1, 1)
			326.0991(1, 2)	292.5905(1, 2)	271.0822(1, 2)	244.8027(1, 2)
			514.4727(3, 1)	440.7149(3, 1)	398.5390(3, 1)	360.8206(3, 1)
120	0.1	0.5	84.7699(1, 1)	71.8978(1, 1)	64.8181(1, 1)	58.8950(1, 1)
			107.2691(2, 1)	91.0149(2, 1)	82.0615(2, 1)	74.5511(2, 1)
			144.2742(3, 1)	122.4904(3, 1)	110.4606(3, 1)	100.3258(3, 1)
		0.7	218.4339(1, 1)	185.2357(1, 1)	166.9869(1, 1)	151.7341(1, 1)
			236.0852(2, 1)	200.2271(2, 1)	180.5073(2, 1)	164.0123(2, 1)
			265.4248(3, 1)	225.1530(3, 1)	202.9894(3, 1)	184.4263(3, 1)
	0.2	0.5	80.1911(1, 1)	68.2982(1, 1)	61.6513(1, 1)	55.9327(1, 1)
			100.2562(2, 1)	85.4855(2, 1)	77.1918(2, 1)	70.0005(2, 1)
			132.2912(3, 1)	113.0043(3, 1)	102.0964(3, 1)	92.5230(3, 1)
		0.7	170.9907(1, 1)	153.4349(1, 1)	142.1771(1, 1)	128.4221(1, 1)
			207.5669(1, 2)	176.6981(1, 2)	159.4778(1, 2)	144.7104(1, 2)
			249.8129(3, 1)	212.8584(3, 1)	192.16309(3, 1)	174.3018(3, 1)
240	0.1	0.5	79.1489(1, 1)	67.1239(1, 1)	60.5129(1, 1)	54.9854(1, 1)
			84.7699(2, 1)	71.8976(2, 1)	64.8181(2, 1)	58.8950(2, 1)
			94.1527(3, 1)	79.8682(3, 1)	72.0069(3, 1)	65.4226(3, 1)
		0.7	214.0167(1, 1)	181.4847(1, 1)	163.6040(1, 1)	148.6617(1, 1)
			218.4339(2, 1)	185.2357(2, 1)	166.9869(2, 1)	151.7341(2, 1)
			225.7922(3, 1)	191.4848(3, 1)	172.6227(3, 1)	156.8523(3, 1)
	0.2	0.5	75.1026(1, 1)	63.9457(1, 1)	57.7174(1, 1)	52.3694(1, 1)
			80.1911(2, 1)	68.2981(2, 1)	61.6512(2, 1)	55.9327(2, 1)
			88.6164(3, 1)	75.5104(3, 1)	68.1711(3, 1)	61.8361(3, 1)
		0.7	140.5909(1, 1)	126.1586(1, 1)	116.9062(1, 1)	105.6009(1, 1)
			170.9907(2, 1)	153.4348(2, 1)	142.1770(2, 1)	128.4221(2, 1)
			207.5669(2, 2)	176.6981(2, 2)	159.4778(2, 2)	144.7103(2, 2)
360	0.1	0.5	78.1096(1, 1)	66.2413(1, 1)	59.7170(1, 1)	54.2626(1, 1)
			80.6049(2, 1)	68.3604(2, 1)	61.6280(2, 1)	55.9981(2, 1)
			84.7699(3, 1)	71.8976(3, 1)	64.8181(3, 1)	58.8950(3, 1)
		0.7	213.1985(1, 1)	180.7898(1, 1)	162.9773(1, 1)	148.0925(1, 1)
			215.1621(2, 1)	182.4572(2, 1)	164.4811(2, 1)	149.4584(2, 1)
			218.4339(3, 1)	185.2357(3, 1)	166.9869(3, 1)	151.7341(3, 1)
	0.2	0.5	74.1583(1, 1)	63.1382(1, 1)	56.9877(1, 1)	51.7083(1, 1)
			76.4236(2, 1)	65.0754(2, 1)	58.7384(2, 1)	53.2944(2, 1)
			80.1910(3, 1)	68.2982(3, 1)	61.6513(3, 1)	55.9327(3, 1)
		0.7	134.2075(1, 1)	120.4308(1, 1)	111.5990(1, 1)	100.8076(1, 1)
			149.0691(2, 1)	133.7658(2, 1)	123.9546(2, 1)	111.9665(2, 1)
			170.9907(3, 1)	153.4348(3, 1)	142.1770(3, 1)	128.4221(3, 1)

the stiffness of the *SSCF* annular sector becomes higher than *SSFS* for $\beta > 150°$; therefore, the value of the natural frequency for *SSCF* plate is higher than that of the *SSFS* plate for $\beta > 150°$.

The variation of the fundamental frequency for *SSFC* versus the variation of the sector angle is depicted in Fig. 4 for some aspect ratios. It can be seen that by increasing the aspect ratio the value of the fundamental frequency decreases expect for higher values of the aspect ratio. It is noticeable that the natural frequency for $a/b = 0.7$ increases slowly with increasing the sector angle for $\beta > 120°$. It can be also seen that the effect of the sector angle on the natural frequency of FG annular sector plates with $a/b = 0.9$ is not significant.

Figure 5 presents the variation of the fundamental frequency versus the power law index for all possible boundary conditions. It can be seen that for all boundary conditions the variation of the fundamental frequency with respect to the power law index is negligible for $n > 2$.

Table 5 Frequency parameters, $\varpi = \omega b^2\sqrt{\frac{\rho_m h}{D_m}}$, of an *SSCS* FG annular sector plate for the third mode sequence number and for some values of n, β, h/c, and a/b

β (deg)	h/c	a/b	$n = 0$	$n = 0.5$	$n = 1$	$n = 2$
45	0.1	0.5	150.9379(1, 1)	128.3682(1, 1)	115.8541(1, 1)	105.2113(1, 1)
			283.3223(2, 1)	241.2097(2, 1)	217.7174(2, 1)	197.5629(2, 1)
			433.6236(1, 3)	323.4759(1, 3)	360.4852(1, 3)	325.5541(1, 3)
		0.7	346.6504(1, 1)	294.7419(1, 1)	266.0034(1, 1)	241.6175(1, 1)
			443.3784(2, 1)	377.1091(2, 1)	340.3519(2, 1)	309.0742(2, 1)
			618.1784(3, 1)	526.0757(3, 1)	474.8321(3, 1)	431.0282(3, 1)
	0.2	0.5	134.0670(1, 1)	114.9524(1, 1)	104.0518(1, 1)	94.2775(1, 1)
			216.8118(1, 2)	194.4652(1, 2)	180.0672(1, 2)	162.4781(1, 2)
			311.4179(1, 3)	269.5536(1, 3)	244.8422(1, 3)	221.2520(1, 3)
		0.7	309.6549(1, 1)	265.5988(1, 1)	240.5146(1, 1)	218.0318(1, 1)
			392.4712(2, 1)	336.6637(2, 1)	304.7893(2, 1)	276.1328(2, 1)
			537.7320(3, 1)	461.7236(3, 1)	418.0145(3, 1)	378.3776(3, 1)
120	0.1	0.5	117.4119(1, 1)	99.8332(1, 1)	90.1020(1, 1)	81.8447(1, 1)
			133.1709(2, 1)	113.2492(2, 1)	102.2114(2, 1)	92.8327(2, 1)
			162.1864(3, 1)	137.9406(3, 1)	124.4914(3, 1)	113.0472(3, 1)
		0.7	321.4748(1, 1)	273.2978(1, 1)	246.6426(1, 1)	224.0486(1, 1)
			333.6416(2, 1)	283.6623(2, 1)	256.0007(2, 1)	232.5407(2, 1)
			354.7228(3, 1)	301.6164(3, 1)	272.2094(3, 1)	247.2489(3, 1)
	0.2	0.5	104.8706(1, 1)	89.9650(1, 1)	81.4784(1, 1)	73.8673(1, 1)
			118.5861(2, 1)	101.7009(2, 1)	92.0809(2, 1)	83.4548(2, 1)
			143.7905(3, 1)	123.2859(3, 1)	111.5829(3, 1)	101.0841(1, 1)
		0.7	288.1295(1, 1)	247.1232(1, 1)	223.7981(1, 1)	202.9164(1, 1)
			298.5123(2, 1)	256.0372(2, 1)	231.8645(2, 1)	210.2102(2, 1)
			316.5817(3, 1)	271.5414(3, 1)	245.8898(3, 1)	222.8920(3, 1)
240	0.1	0.5	113.7661(1, 1)	96.7273(1, 1)	87.2977(1, 1)	79.3000(1, 1)
			117.4119(2, 1)	99.8332(2, 1)	90.1021(2, 1)	81.8446(2, 1)
			123.7713(3, 1)	105.2485(3, 1)	94.9905(3, 1)	86.2806(3, 1)
		0.7	318.4965(1, 1)	270.7604(1, 1)	244.3514(1, 1)	221.9694(1, 1)
			321.4747(2, 1)	273.2978(2, 1)	246.6426(2, 1)	224.0487(2, 1)
			326.4963(3, 1)	277.5757(3, 1)	250.5053(3, 1)	227.5538(3, 1)
	0.2	0.5	101.7348(1, 1)	87.2789(1, 1)	79.0504(1, 1)	71.6718(1, 1)
			104.8706(2, 1)	89.9650(2, 1)	81.4785(2, 1)	73.8673(2, 1)
			110.3861(3, 1)	94.6856(3, 1)	85.7439(3, 1)	77.7245(3, 1)
		0.7	285.5963(1, 1)	244.9474(1, 1)	221.8287(1, 1)	201.1356(1, 1)
			288.1295(2, 1)	247.1232(2, 1)	223.7981(2, 1)	202.9164(2, 1)
			292.4088(3, 1)	250.7977(3, 1)	227.1236(3, 1)	205.9234(3, 1)
360	0.1	0.5	113.1064(1, 1)	96.1652(1, 1)	86.7901(1, 1)	78.8394(1, 1)
			114.6980(2, 1)	97.5213(2, 1)	88.0147(2, 1)	79.9506(2, 1)
			117.4120(3, 1)	99.8332(3, 1)	90.1021(3, 1)	81.8447(3, 1)
		0.7	317.9479(1, 1)	270.2930(1, 1)	243.9293(1, 1)	221.5864(1, 1)
			319.2661(2, 1)	271.4161(2, 1)	244.9434(2, 1)	222.5067(2, 1)
			321.4748(3, 1)	273.2978(3, 1)	246.6426(3, 1)	224.0487(3, 1)
	0.2	0.5	101.1704(1, 1)	86.7951(1, 1)	78.6129(1, 1)	71.2763(1, 1)
			102.5339(2, 1)	87.9636(2, 1)	79.6694(2, 1)	72.2316(2, 1)
			104.8706(3, 1)	89.9650(3, 1)	81.4785(3, 1)	73.8673(3, 1)
		0.7	285.1302(1, 1)	244.5469(1, 1)	221.4663(1, 1)	200.8079(1, 1)
			286.2506(2, 1)	245.5093(2, 1)	222.3374(2, 1)	201.5956(2, 1)
			288.1296(3, 1)	247.1232(3, 1)	223.7981(3, 1)	202.9164(3, 1)

Figure 6 shows the variation of the fundamental frequency for *SSCF* FG annular sector plates versus the variation of the aspect ratio for different values of the power law index. It can be seen that by increasing the aspect ratio, the value of the fundamental frequency decreases for $a/b < 0.4$ and increases for $a/b > 0.4$.

The variation of the fundamental frequency for all boundary conditions versus the variation of the thickness/length ratio is depicted in Fig. 7. It is observed that by increasing the value of the thickness/length ratio, the fundamental frequency increases for all boundary conditions. It is obvious because increasing the thickness causes to increase the stiffness of the FG annular sector plate.

Figure 8 shows the variation of the fundamental frequency for an *SSFC* FG annular sector plates versus the variation of the sector angle for different power law indices. It can be seen that the change of the natural frequency is rapid for sector angles less than 90°, and the variation of frequency is very small for $\beta > 180°$.

Table 6 Frequency parameters, $\varpi = \omega b^2\sqrt{\frac{\rho_m h}{D_m}}$, of an *SSSC* FG annular sector plate for the third mode sequence number and for some values of n, β, h/c, and a/b

β (deg)	h/c	a/b	$n = 0$	$n = 0.5$	$n = 1$	$n = 2$
45	0.1	0.5	167.3939(1, 1)	142.4141(1, 1)	128.5500(1, 1)	116.7361(1, 1)
			311.1625(2, 1)	265.3282(2, 1)	239.6548(2, 1)	217.4329(2, 1)
			522.7930(3, 1)	447.2098(3, 1)	404.3430(3, 1)	366.4320(3, 1)
		0.7	362.0187(1, 1)	307.8012(1, 1)	277.7866(1, 1)	252.3221(1, 1)
			468.4060(2, 1)	398.4847(2, 1)	359.6781(2, 1)	326.6161(2, 1)
			653.6671(3, 1)	556.6098(3, 1)	502.5237(3, 1)	456.1347(3, 1)
	0.2	0.5	147.0731(1, 1)	126.3214(1, 1)	114.4357(1, 1)	103.6788(1, 1)
			258.8138(2, 1)	223.2097(2, 1)	202.4356(2, 1)	183.0668(2, 1)
			343.0312(1, 3)	307.4912(1, 3)	284.4289(1, 3)	256.2776(1, 3)
		0.7	323.4015(1, 1)	277.4221(1, 1)	251.2402(1, 1)	227.7667(1, 1)
			411.9878(2, 1)	353.7497(2, 1)	320.4051(2, 1)	290.2678(2, 1)
			561.1319(3, 1)	482.6244(3, 1)	437.2891(3, 1)	395.7817(3, 1)
120	0.1	0.5	126.8383(1, 1)	107.8360(1, 1)	97.3202(1, 1)	88.4033(1, 1)
			146.3778(2, 1)	124.4917(2, 1)	112.3622(2, 1)	102.0514(2, 1)
			180.3252(3, 1)	153.4470(3, 1)	138.5165(3, 1)	125.7756(3, 1)
		0.7	333.4239(1, 1)	283.4355(1, 1)	255.7840(1, 1)	232.3561(1, 1)
			347.3084(2, 1)	295.2665(2, 1)	266.4676(2, 1)	242.0510(2, 1)
			371.0850(3, 1)	315.5270(3, 1)	284.7629(3, 1)	258.6523(3, 1)
	0.2	0.5	113.5391(1, 1)	97.3938(1, 1)	88.2078(1, 1)	79.9792(1, 1)
			129.7848(2, 1)	111.4028(2, 1)	100.9082(2, 1)	91.4573(2, 1)
			157.5910(3, 1)	135.4060(3, 1)	122.6755(3, 1)	111.1208(3, 1)
		0.7	299.3834(1, 1)	256.7352(1, 1)	232.4937(1, 1)	210.8195(1, 1)
			311.0465(2, 1)	266.7815(2, 1)	241.5982(2, 1)	219.0505(2, 1)
			331.0102(3, 1)	283.9747(3, 1)	257.1775(3, 1)	233.1336(3, 1)
240	0.1	0.5	122.1422(1, 1)	103.8336(1, 1)	93.7056(1, 1)	85.1233(1, 1)
			126.8384(2, 1)	107.8360(2, 1)	97.3202(2, 1)	88.4033(2, 1)
			134.8547(3, 1)	114.6686(3, 1)	103.4907(3, 1)	94.0023(3, 1)
		0.7	330.0045(1, 1)	280.5218(1, 1)	253.1528(1, 1)	229.9683(1, 1)
			333.4239(2, 1)	283.4355(2, 1)	255.7840(2, 1)	232.3560(2, 1)
			339.1703(3, 1)	288.3320(3, 1)	260.2057(3, 1)	236.3685(3, 1)
	0.2	0.5	109.6224(1, 1)	94.0163(1, 1)	85.1455(1, 1)	77.2113(1, 1)
			113.5392(2, 1)	97.3938(2, 1)	88.2078(2, 1)	79.9792(2, 1)
			120.2184(3, 1)	103.1531(3, 1)	93.4291(3, 1)	84.6983(3, 1)
		0.7	296.5124(1, 1)	254.2616(1, 1)	230.2518(1, 1)	208.7927(1, 1)
			299.3835(2, 1)	256.7351(2, 1)	232.4937(2, 1)	210.8195(2, 1)
			304.2098(3, 1)	260.8928(3, 1)	236.2617(3, 1)	214.2260(3, 1)
360	0.1	0.5	121.2835(1, 1)	103.1017(1, 1)	93.0446(1, 1)	84.5235(1, 1)
			123.3504(2, 1)	104.8633(2, 1)	94.6355(2, 1)	85.9671(2, 1)
			126.8384(3, 1)	107.8360(3, 1)	97.3201(3, 1)	88.4033(3, 1)
		0.7	329.3737(1, 1)	279.9842(1, 1)	252.6674(1, 1)	229.5278(1, 1)
			330.8889(2, 1)	281.2753(2, 1)	253.8333(2, 1)	230.5859(2, 1)
			333.4239(3, 1)	283.4355(3, 1)	255.7840(3, 1)	232.3561(3, 1)
	0.2	0.5	108.9062(1, 1)	93.3986(1, 1)	84.5854(1, 1)	76.7051(1, 1)
			110.6301(2, 1)	94.8853(2, 1)	85.9335(2, 1)	77.9234(2, 1)
			113.5392(3, 1)	97.3938(3, 1)	88.2078(3, 1)	79.9792(3, 1)
		0.7	295.9828(1, 1)	253.8053(1, 1)	229.8382(1, 1)	208.4188(1, 1)
			297.2549(2, 1)	254.9013(2, 1)	230.8316(2, 1)	209.3169(2, 1)
			299.3834(3, 1)	256.7352(3, 1)	232.4936(3, 1)	210.8195(3, 1)

The mode shape contour plots of an FG annular sector plate with $\beta = 90°$ for all nine possible boundary conditions are shown in Fig. 9. It can be seen that the wave number is different for various boundary conditions.

7 Conclusions

The aim of this paper is to present a benchmark solution for the free vibration analysis of moderately thick functionally graded annular sector plates. The governing equations of motion have been derived based on the first-order shear deformation plate theory. These equations are five highly coupled partial differential equations that have been decoupled by some mathematical manipulations. The decoupled equations have been solved analytically for the FG annular sector plates with various boundary conditions in circular edges. By satisfying the boundary conditions at the inner and outer radii, the eigenvalue problem for finding the natural frequency

Table 7 Frequency parameters, $\varpi = \omega b^2\sqrt{\frac{\rho_m h}{D_m}}$, of an *SSFC* FG annular sector plate for the third mode sequence number and for some values of n, β, h/c, and a/b

β (deg)	h/c	a/b	$n=0$	$n=0.5$	$n=1$	$n=2$
45	0.1	0.5	118.9598(1, 1)	101.0694(1, 1)	91.1831(1, 1)	82.8283(1, 1)
			256.1909(1, 2)	218.3877(1, 2)	197.2246(1, 2)	178.9260(1, 2)
			458.8287(2, 2)	392.1713(2, 2)	354.4849(2, 2)	321.3338(2, 2)
		0.7	141.2127(1, 1)	119.8266(1, 1)	108.0613(1, 1)	98.1970(1, 1)
			290.9851(2, 1)	247.1182(2, 1)	222.9050(2, 1)	202.4911(2, 1)
			524.1364(3, 1)	445.6823(3, 1)	402.1518(3, 1)	365.1322(3, 1)
	0.2	0.5	108.2120(1, 1)	92.5848(1, 1)	83.7404(1, 1)	75.9238(1, 1)
			214.3380(1, 2)	184.5260(1, 2)	167.0962(1, 2)	150.8898(1, 2)
			264.9674(1, 3)	237.7363(1, 3)	220.2169(1, 3)	198.8343(1, 3)
		0.7	133.4912(1, 1)	113.7256(1, 1)	102.7014(1, 1)	93.2174(1, 1)
			267.5887(2, 1)	228.6011(2, 1)	206.6168(2, 1)	187.3474(2, 1)
			464.2108(3, 1)	397.9451(3, 1)	360.0495(3, 1)	326.0454(3, 1)
120	0.1	0.5	50.5555(1, 1)	42.9043(1, 1)	38.6944(1, 1)	35.1626(1, 1)
			86.7640(2, 1)	73.6840(2, 1)	66.4694(2, 1)	60.3904(2, 1)
			137.3478(3, 1)	116.7247(3, 1)	105.3151(3, 1)	95.6545(3, 1)
		0.7	92.8550(1, 1)	78.7156(1, 1)	70.9579(1, 1)	64.4910(1, 1)
			117.4017(2, 1)	99.5907(2, 1)	89.8014(2, 1)	81.6092(2, 1)
			155.1970(3, 1)	131.7085(3, 1)	118.7817(3, 1)	107.9351(3, 1)
	0.2	0.5	47.7369(1, 1)	40.6771(1, 1)	36.7395(1, 1)	33.3492(1, 1)
			80.1289(2, 1)	68.4532(2, 1)	61.8850(2, 1)	56.1389(2, 1)
			123.8530(3, 1)	106.0543(3, 1)	95.9475(3, 1)	86.9651(3, 1)
		0.7	89.7252(1, 1)	76.2527(1, 1)	68.7919(1, 1)	62.4684(1, 1)
			111.8619(2, 1)	95.2152(2, 1)	85.9562(2, 1)	78.0341(2, 1)
			146.2020(3, 1)	124.6014(3, 1)	112.5380(3, 1)	102.1347(3, 1)
240	0.1	0.5	38.9707(1, 1)	33.0463(1, 1)	29.79331(1, 1)	27.0768(1, 1)
			50.5555(2, 1)	42.9042(2, 1)	38.6944(2, 1)	35.1626(2, 1)
			66.7857(3, 1)	56.7022(3, 1)	51.1466(3, 1)	46.4739(3, 1)
		0.7	86.3045(1, 1)	73.1406(1, 1)	65.9234(1, 1)	59.9177(1, 1)
			92.8549(2, 1)	78.7156(2, 1)	70.9579(2, 1)	64.4911(2, 1)
			103.3492(3, 1)	87.6427(3, 1)	79.0174(3, 1)	71.8125(3, 1)
	0.2	0.5	37.4194(1, 1)	31.8241(1, 1)	28.7194(1, 1)	26.0765(1, 1)
			47.7369(2, 1)	40.6772(2, 1)	36.7395(2, 1)	33.3492(2, 1)
			62.3090(3, 1)	53.1696(3, 1)	48.0494(3, 1)	43.6027(3, 1)
		0.7	83.8805(1, 1)	71.2399(1, 1)	64.2514(1, 1)	58.3506(1, 1)
			89.7251(2, 1)	76.2528(2, 1)	68.7919(2, 1)	62.4684(2, 1)
			99.1538(3, 1)	84.3330(3, 1)	76.1078(3, 1)	69.1030(3, 1)
360	0.1	0.5	36.5306(1, 1)	30.9679(1, 1)	27.9157(1, 1)	25.3714(1, 1)
			42.1971(2, 1)	35.7932(2, 1)	32.2742(2, 1)	29.3305(2, 1)
			50.5555(3, 1)	42.9042(3, 1)	38.6944(3, 1)	35.16263(3, 1)
		0.7	85.0657(1, 1)	72.0859(1, 1)	64.9709(1, 1)	59.0525(1, 1)
			88.0245(2, 1)	74.6047(2, 1)	67.2457(2, 1)	61.1189(2, 1)
			92.8550(3, 1)	78.7156(3, 1)	70.9579(3, 1)	64.4911(3, 1)
	0.2	0.5	35.2723(1, 1)	29.9795(1, 1)	27.0472(1, 1)	24.5602(1, 1)
			40.2758(2, 1)	34.2766(2, 1)	30.9419(2, 1)	28.0920(2, 1)
			47.7369(3, 1)	40.6771(3, 1)	36.7395(3, 1)	33.3493(3, 1)
		0.7	82.7796(1, 1)	70.2953(1, 1)	63.3956(1, 1)	57.5745(1, 1)
			85.4115(2, 1)	72.5534(2, 1)	65.4413(2, 1)	59.4298(2, 1)
			89.7252(3, 1)	76.2528(3, 1)	68.7919(3, 1)	62.4684(3, 1)

has been obtained. The natural frequencies of the annular sector plate for nine different boundary conditions with several aspect ratios, different thickness/length ratios, and some power law indices have been tabulated. The following conclusions can be remarked

(i) As the power law index increases, the natural frequencies of the FG annular sector plate decrease for all wave numbers.
(ii) The variations of the thickness, aspect ratio, sector angle, and boundary conditions of the FG annular sector plates can change the wave number.
(iii) The value of the fundamental frequency decreases by increasing the aspect ratio up to a point and then it starts increasing by further increase in the aspect ratio except for *SSFS* and *SSFF* boundary conditions, where the fundamental frequency decreases by increasing the aspect ratio.

Table 8 Frequency parameters, $\varpi = \omega b^2\sqrt{\frac{\rho_m h}{D_m}}$, of an *SSCF* FG annular sector plate for the third mode sequence number and for some values of n, β, h/c, and a/b

β (deg)	h/c	a/b	$n=0$	$n=0.5$	$n=1$	$n=2$
45	0.1	0.5	49.0105(1, 1)	41.5772(1, 1)	37.4886(1, 1)	34.0641(1, 1)
			154.2382(2, 1)	130.9958(2, 1)	118.1335(2, 1)	107.2612(2, 1)
			318.5869(3, 1)	271.2686(3, 1)	244.7965(3, 1)	222.0162(3, 1)
		0.7	92.5463(1, 1)	78.4880(1, 1)	70.7658(1, 1)	64.3125(1, 1)
			181.2412(2, 1)	153.7814(2, 1)	138.6654(2, 1)	125.9880(2, 1)
			344.4623(3, 1)	292.4713(3, 1)	263.7541(3, 1)	239.5441(3, 1)
	0.2	0.5	46.5133(1, 1)	39.5825(1, 1)	35.7208(1, 1)	32.4131(1, 1)
			139.9757(2, 1)	119.5480(2, 1)	107.9430(2, 1)	97.7204(2, 1)
			216.4691(1, 3)	194.3784(1, 3)	180.2821(1, 3)	163.0698(2, 1)
		0.7	88.54049(1, 1)	75.3320(1, 1)	67.9941(1, 1)	61.7316(1, 1)
			170.8016(2, 1)	145.4652(2, 1)	131.3047(2, 1)	119.1131(2, 1)
			316.5195(3, 1)	270.1361(3, 1)	243.9330(3, 1)	221.0111(3, 1)
120	0.1	0.5	26.6606(1, 1)	22.6047(1, 1)	20.3788(1, 1)	18.5218(1, 1)
			35.6109(2, 1)	30.2100(2, 1)	27.2406(2, 1)	24.7547(2, 1)
			57.9539(3, 1)	49.1646(3, 1)	44.3286(3, 1)	40.2768(3, 1)
		0.7	74.3077(1, 1)	62.9771(1, 1)	56.7652(1, 1)	51.5951(1, 1)
			82.4431(2, 1)	69.9011(2, 1)	63.0172(2, 1)	57.2737(2, 1)
			99.2963(3, 1)	84.2212(3, 1)	75.9378(3, 1)	69.0108(3, 1)
	0.2	0.5	25.6532(1, 1)	21.8178(1, 1)	19.6911(1, 1)	17.8817(1, 1)
			33.8538(2, 1)	28.8172(2, 1)	26.0138(2, 1)	23.6128(2, 1)
			54.8940(3, 1)	46.7160(3, 1)	42.1541(3, 1)	38.2425(3, 1)
		0.7	72.1862(1, 1)	61.3201(1, 1)	55.3131(1, 1)	50.2378(1, 1)
			79.3483(2, 1)	67.4720(2, 1)	60.8869(2, 1)	55.2886(2, 1)
			94.7658(3, 1)	80.6452(3, 1)	72.7942(3, 1)	66.0838(3, 1)
240	0.1	0.5	25.5951(1, 1)	21.6933(1, 1)	19.5541(1, 1)	17.7734(1, 1)
			26.6606(2, 1)	22.6047(2, 1)	20.3788(2, 1)	18.5219(2, 1)
			29.6337(3, 1)	25.1351(3, 1)	22.6634(3, 1)	20.5967(3, 1)
		0.7	72.5851(1, 1)	61.5088(1, 1)	55.4384(1, 1)	50.3903(1, 1)
			74.3077(2, 1)	62.9771(2, 1)	56.7652(2, 1)	51.5951(2, 1)
			77.4712(3, 1)	65.6712(3, 1)	59.1984(3, 1)	53.8051(3, 1)
	0.2	0.5	24.8404(1, 1)	21.1063(1, 1)	19.0414(1, 1)	17.2951(1, 1)
			25.6533(2, 1)	21.8178(2, 1)	19.6911(2, 1)	17.8817(2, 1)
			28.2765(3, 1)	24.0676(3, 1)	21.7277(3, 1)	19.7266(3, 1)
		0.7	70.7253(1, 1)	60.0587(1, 1)	54.1676(1, 1)	49.2005(1, 1)
			72.1862(2, 1)	61.3201(2, 1)	55.3131(2, 1)	50.2378(2, 1)
			74.9304(3, 1)	63.6821(3, 1)	57.4551(3, 1)	52.1783(3, 1)
360	0.1	0.5	25.4653(1, 1)	21.5816(1, 1)	19.4527(1, 1)	17.6815(1, 1)
			25.8131(2, 1)	21.8804(2, 1)	19.7236(2, 1)	17.9271(2, 1)
			26.6606(3, 1)	22.6047(3, 1)	20.3788(3, 1)	18.5218(3, 1)
		0.7	72.2815(1, 1)	61.2499(1, 1)	55.2045(1, 1)	50.1778(1, 1)
			73.0183(2, 1)	61.8782(2, 1)	55.7723(2, 1)	50.6935(2, 1)
			74.3078(3, 1)	62.9771(3, 1)	56.7652(3, 1)	51.5952(3, 1)
	0.2	0.5	24.7610(1, 1)	21.0343(1, 1)	18.9748(1, 1)	17.2352(1, 1)
			24.9897(2, 1)	21.2393(2, 1)	19.1636(2, 1)	17.4051(2, 1)
			25.6533(3, 1)	21.8179(3, 1)	19.6911(3, 1)	17.8817(3, 1)
		0.7	70.4710(1, 1)	59.8388(1, 1)	53.9677(1, 1)	49.0195(1, 1)
			71.0899(2, 1)	60.3739(2, 1)	54.4539(2, 1)	49.4597(2, 1)
			72.1862(3, 1)	61.3201(3, 1)	55.3131(3, 1)	50.2378(3, 1)

(iv) For $a/b < 0.2$, the variation of the natural frequencies for FG annular sector plates with the same boundary condition in the outer circular edge is negligible.

(v) For $\beta < 60^\circ$, the value of the fundamental natural frequency decreases rapidly with increasing sector angle, whereas the variation of the fundamental frequency is very small for $\beta > 60^\circ$. However, for annular sector plates with *SSCF* boundary condition, the value of the fundamental frequency decreases in the first part and then increases with increasing the sector angle.

(vi) By increasing the aspect ratio, the value of the fundamental frequency decreases. Also, the effect of the sector angle on the natural frequencies of FG annular sector plates with $a/b > 0.7$ is negligible.

(vii) The variation of the fundamental frequency versus the power law index is negligible for $n > 2$ in all boundary conditions.

(viii) For FG annular sector plates with free outer edge, by increasing the aspect ratio, the value of the fundamental frequency decreases for $a/b < 0.4$ and then increases for $a/b > 0.4$.

Table 9 Frequency parameters, $\varpi = \omega b^2\sqrt{\frac{\rho_m h}{D_m}}$, of an *SSFS* FG annular sector plate for the third mode sequence number and for some values of n, β, h/c, and a/b

β (deg)	h/c	a/b	$n=0$	$n=0.5$	$n=1$	$n=2$
45	0.1	0.5	99.7196(1, 1)	84.6083(1, 1)	76.2868(1, 1)	69.3081(1, 1)
			217.3898(1, 2)	184.9009(1, 2)	166.8277(1, 2)	151.4036(1, 2)
			302.6726(1, 3)	271.5912(1, 3)	251.6537(1, 3)	227.2954(1, 3)
		0.7	99.5767(1, 1)	84.4280(1, 1)	76.1133(1, 1)	69.1745(1, 1)
			257.0821(2, 1)	218.1137(2, 1)	196.6597(2, 1)	178.6730(2, 1)
			399.7664(1, 3)	339.4000(1, 3)	306.0636(1, 3)	277.9557(1, 3)
	0.2	0.5	93.4142(1, 1)	79.6377(1, 1)	71.9111(1, 1)	65.2215(1, 1)
			151.3363(1, 2)	135.7526(1, 2)	125.7158(1, 2)	113.4596(1, 2)
			190.4394(1, 3)	163.2110(1, 3)	147.5845(1, 3)	133.5282(1, 3)
		0.7	96.0711(1, 1)	81.6414(1, 1)	73.6486(1, 1)	66.8712(1, 1)
			163.2375(1, 2)	146.4870(1, 2)	135.7521(1, 2)	122.6364(1, 2)
			365.0708(1, 3)	311.3908(1, 3)	280.9583(1, 3)	254.3271(1, 3)
120	0.1	0.5	31.9926(1, 1)	27.1332(1, 1)	24.4646(1, 1)	22.2342(1, 1)
			68.5279(2, 1)	58.1224(2, 1)	52.4021(2, 1)	47.6175(2, 1)
			117.3930(3, 1)	99.6294(3, 1)	89.8365(3, 1)	81.6088(3, 1)
		0.7	35.7431(1, 1)	30.3013(1, 1)	27.3166(1, 1)	24.8285(1, 1)
			71.3798(2, 1)	60.5184(2, 1)	54.5586(2, 1)	49.5866(2, 1)
			115.1962(3, 1)	97.6747(3, 1)	88.0553(3, 1)	80.0259(3, 1)
	0.2	0.5	30.7569(1, 1)	26.1461(1, 1)	23.5896(1, 1)	21.4153(1, 1)
			36.6187(1, 2)	32.8665(1, 2)	30.4652(1, 2)	27.5319(1, 2)
			109.0146(3, 1)	93.0152(3, 1)	84.0110(3, 1)	76.1711(3, 1)
		0.7	34.7831(1, 1)	29.5280(1, 1)	26.6288(1, 1)	24.1871(1, 1)
			69.1115(2, 1)	58.7019(2, 1)	52.9436(1, 2)	48.0715(1, 2)
			86.9502(2, 2)	78.0404(2, 2)	72.3386(2, 2)	65.3733(2, 2)
240	0.1	0.5	17.8297(1, 1)	15.1185(1, 1)	13.6306(1, 1)	12.3887(1, 1)
			31.9925(2, 1)	27.1332(2, 1)	24.4646(2, 1)	22.2341(2, 1)
			48.8239(3, 1)	41.4066(3, 1)	37.3321(3, 1)	33.9266(3, 1)
		0.7	21.2108(1, 1)	17.9751(1, 1)	16.2021(1, 1)	14.7271(1, 1)
			35.7431(2, 1)	30.3013(2, 1)	27.3167(2, 1)	24.8286(2, 1)
			52.6247(3, 1)	44.6159(3, 1)	40.2221(3, 1)	36.5574(3, 1)
	0.2	0.5	17.2719(1, 1)	14.6701(1, 1)	13.2329(1, 1)	12.0189(1, 1)
			30.7569(2, 1)	26.1461(2, 1)	23.5896(2, 1)	21.4153(2, 1)
			46.7349(3, 1)	39.7506(3, 1)	35.8689(3, 1)	32.5551(3, 1)
		0.7	20.7932(1, 1)	17.6368(1, 1)	15.8998(1, 1)	14.4444(1, 1)
			34.7831(2, 1)	29.5280(2, 1)	26.6288(2, 1)	24.1871(2, 1)
			51.0653(3, 1)	43.3528(3, 1)	39.0886(3, 1)	35.4803(3, 1)
360	0.1	0.5	13.9811(1, 1)	11.8508(1, 1)	10.6829(1, 1)	9.71001(1, 1)
			22.2137(2, 1)	18.8387(2, 1)	16.9858(2, 1)	15.4378(2, 1)
			31.9925(3, 1)	27.1333(3, 1)	24.4646(3, 1)	22.2341(3, 1)
		0.7	17.3823(1, 1)	14.7265(1, 1)	13.2722(1, 1)	12.0643(1, 1)
			25.6836(2, 1)	21.7695(2, 1)	19.6238(2, 1)	17.8368(2, 1)
			35.7431(3, 1)	30.3013(3, 1)	27.3166(3, 1)	24.8286(3, 1)
	0.2	0.5	13.6402(1, 1)	11.5757(1, 1)	10.4379(1, 1)	9.4814(1, 1)
			21.4351(2, 1)	18.2147(2, 1)	16.4333(2, 1)	14.9243(2, 1)
			30.7569(3, 1)	26.1461(3, 1)	23.5896(3, 1)	21.4154(3, 1)
		0.7	17.1299(1, 1)	14.5210(1, 1)	13.0872(1, 1)	11.8901(1, 1)
			25.0899(2, 1)	21.2900(2, 1)	19.1965(2, 1)	17.4384(2, 1)
			34.7831(3, 1)	29.5280(3, 1)	26.6288(3, 1)	24.1871(3, 1)

Appendix

Explicit relations for the functions φ_1, φ_2, φ_3, rotations functions, and in-plane displacements:

$$\begin{aligned}\varphi_{1m}(r) = {} & \frac{\hat{D}\lambda_1^2 - K_2 J_1\omega_m^2 - K_1 J_1\lambda_1\omega_m^2}{J_1\omega_m^2}\left(C_1 I_{\mu_m}\left(\sqrt{-\lambda_1}r\right) + C_2 K_{\mu_m}\left(\sqrt{-\lambda_1}r\right)\right)\\ & + \frac{\hat{D}\lambda_2^2 - K_2 J_1\omega_m^2 - K_1 J_1\lambda_2\omega_m^2}{J_1\omega_m^2}\left(C_3 J_{\mu_m}\left(\sqrt{\lambda_2}r\right) + C_4 Y_{\mu_m}\left(\sqrt{\lambda_2}r\right)\right)\\ & + \frac{\hat{D}\lambda_3^2 - K_2 J_1\omega_m^2 - K_1 J_1\lambda_3\omega_m^2}{J_1\omega_m^2}\left(C_5 J_{\mu_m}\left(\sqrt{\lambda_3}r\right) + C_5 Y_{\mu_m}\left(\sqrt{\lambda_3}r\right)\right),\end{aligned}$$

Table 10 Frequency parameters, $\varpi = \omega b^2\sqrt{\frac{\rho_m h}{D_m}}$, of an *SSSF* FG annular sector plate for the third mode sequence number and for some values of n, β, h/c, and a/b

β (deg)	h/c	a/b	$n=0$	$n=0.5$	$n=1$	$n=2$
45	0.1	0.5	44.0451(1, 1)	37.3336(1, 1)	33.6501(1, 1)	30.5796(1, 1)
			153.8124(2, 1)	130.6250(2, 1)	117.7953(2, 1)	106.9554(2, 1)
			318.5639(3, 1)	271.2481(3, 1)	244.7777(3, 1)	221.9993(3, 1)
		0.7	57.0716(1, 1)	48.3606(1, 1)	43.5872(1, 1)	39.6176(1, 1)
			166.0574(2, 1)	140.8028(2, 1)	126.9257(2, 1)	115.3329(2, 1)
			338.3008(3, 1)	287.1586(3, 1)	258.9315(3, 1)	235.1743(3, 1)
	0.2	0.5	42.5445(1, 1)	36.1337(1, 1)	32.5798(1, 1)	29.5711(1, 1)
			139.7382(2, 1)	119.3350(2, 1)	107.7466(2, 1)	97.5442(2, 1)
			193.1985(1, 3)	173.4527(1, 3)	160.8321(1, 3)	145.4232(1, 3)
		0.7	55.8683(1, 1)	47.3949(1, 1)	42.7257(1, 1)	38.8080(1, 1)
			158.7825(2, 1)	135.0106(2, 1)	121.7818(2, 1)	110.5016(2, 1)
			312.4788(3, 1)	266.5548(3, 1)	240.6466(3, 1)	218.0522(3, 1)
120	0.1	0.5	11.8275(1, 1)	10.0188(1, 1)	9.0286(1, 1)	8.2072(1, 1)
			27.2476(3, 1)	23.0888(3, 1)	20.8091(2, 1)	18.9129(2, 1)
			54.1962(3, 1)	45.9464(3, 1)	41.4149(3, 1)	37.6328(3, 1)
		0.7	20.7111(1, 1)	17.5445(1, 1)	15.8112(1, 1)	14.3727(1, 1)
			39.7528(2, 1)	33.6817(2, 1)	30.3564(2, 1)	27.5930(2, 1)
			67.1782(3, 1)	56.9278(3, 1)	51.3094(3, 1)	46.6354(3, 1)
	0.2	0.5	11.6796(1, 1)	9.8995(1, 1)	8.9217(1, 1)	8.1060(1, 1)
			26.6033(2, 1)	22.5721(2, 1)	20.3473(2, 1)	18.4774(2, 1)
			52.0207(3, 1)	44.2078(3, 1)	39.8655(3, 1)	36.1736(3, 1)
		0.7	20.4657(1, 1)	17.3448(1, 1)	15.6314(1, 1)	14.2031(1, 1)
			39.0616(2, 1)	33.1247(2, 1)	29.8583(2, 1)	27.1250(2, 1)
			65.6192(3, 1)	55.6790(3, 1)	50.1964(3, 1)	45.5892(3, 1)
240	0.1	0.5	8.8301(1, 1)	7.4783(1, 1)	6.7387(1, 1)	6.1258(1, 1)
			11.8274(2, 1)	10.0187(2, 1)	9.0286(2, 1)	8.20716(2, 1)
			17.9692(3, 1)	15.2238(3, 1)	13.7201(3, 1)	12.4709(3, 1)
		0.7	14.5991(1, 1)	12.3642(1, 1)	11.1416(1, 1)	10.1282(1, 1)
			20.7111(2, 1)	17.5445(2, 1)	15.8112(2, 1)	14.3727(2, 1)
			29.2026(3, 1)	24.7408(3, 1)	22.2976(3, 1)	20.2684(3, 1)
	0.2	0.5	8.7620(1, 1)	7.4232(1, 1)	6.6889(1, 1)	6.0783(1, 1)
			11.6796(2, 1)	9.8995(2, 1)	8.9217(2, 1)	8.1060(2, 1)
			17.6539(3, 1)	14.9703(3, 1)	13.4931(3, 1)	12.2566(3, 1)
		0.7	14.4904(1, 1)	12.2747(1, 1)	11.0599(1, 1)	10.0502(1, 1)
			20.4657(2, 1)	17.3448(2, 1)	15.6314(2, 1)	14.2031(2, 1)
			28.7694(3, 1)	24.3902(3, 1)	21.9834(3, 1)	19.9730(3, 1)
360	0.1	0.5	8.3967(1, 1)	7.1107(1, 1)	6.4074(1, 1)	5.8247(1, 1)
			9.5148(2, 1)	8.0587(2, 1)	7.2619(2, 1)	6.6014(2, 1)
			11.8275(3, 1)	10.0187(3, 1)	9.0287(3, 1)	8.2072(2, 1)
		0.7	13.2794(1, 1)	11.2455(1, 1)	10.1331(1, 1)	9.21156(1, 1)
			16.3189(2, 1)	13.8220(2, 1)	12.4557(2, 1)	11.3227(2, 1)
			20.7112(3, 1)	17.5445(3, 1)	15.8112(3, 1)	14.3727(3, 1)
	0.2	0.5	8.3423(1, 1)	7.06673(1, 1)	6.3674(1, 1)	5.7863(1, 1)
			9.4270(2, 1)	7.9878(2, 1)	7.1981(2, 1)	6.5407(2, 1)
			11.6796(3, 1)	9.8996(3, 1)	8.9217(3, 1)	8.1060(3, 1)
		0.7	13.2028(1, 1)	11.1819(1, 1)	10.0744(1, 1)	9.1549(1, 1)
			16.1705(2, 1)	13.7004(2, 1)	12.3455(2, 1)	11.2181(2, 1)
			20.4657(3, 1)	17.3449(3, 1)	15.6314(3, 1)	14.2031(3, 1)

$$\varphi_{2m}(r) = \frac{\left(k^2 A_{33} + \hat{C}\lambda_4^2 - J_2\omega_m^2\right)}{J_1\omega_m^2}\left(C_7 J_{\mu_m}(\lambda_4 r) + C_8 Y_{\mu_m}(\lambda_4 r)\right) + \frac{\left(k^2 A_{33} - \hat{C}\lambda_5^2 - J_2\omega_m^2\right)}{J_1\omega_m^2}\left(C_9 I_{\mu_m}(\lambda_5 r) + C10 K_{\mu_m}(\lambda_5 r)\right),$$

$$\varphi_{3m}(r) = \frac{k^2 A_{33}\lambda_1 - I_0\omega_m^2}{k^2 A_{33}}\left(C_1 I_{\mu_m}\left(\sqrt{-\lambda_1} r\right) + C_2 K_{\mu_m}\left(\sqrt{-\lambda_1} r\right)\right) + \frac{k^2 A_{33}\lambda_2 - I_0\omega_m^2}{k^2 A_{33}}\left(C_3 J_{\mu_m}\left(\sqrt{\lambda_2} r\right) + C_4 Y_{\mu_m}\left(\sqrt{\lambda_2} r\right)\right),$$

Table 11 Frequency parameters, $\varpi = \omega b^2\sqrt{\frac{\rho_m h}{D_m}}$, of an *SSFF* FG annular sector plate for the third mode sequence number and for some values of n, β, h/c, and a/b

β (deg)	h/c	a/b	$n=0$	$n=0.5$	$n=1$	$n=2$
45	0.1	0.5	40.7617(1, 1)	34.5490(1, 1)	31.1401(1, 1)	28.2997(1, 1)
			125.7895(1, 2)	106.8025(1, 2)	96.3091(1, 2)	87.4581(1, 2)
			265.0677(1, 3)	225.4763(1, 3)	203.3517(1, 3)	184.3848(1, 3)
		0.7	36.5248(1, 1)	30.9402(1, 1)	27.8836(1, 1)	25.3474(1, 1)
			141.8086(1, 2)	120.3239(1, 2)	108.4874(1, 2)	98.5487(1, 2)
			303.4384(1, 3)	272.3316(1, 3)	252.4221(1, 3)	228.0950(1, 3)
	0.2	0.5	39.4468(1, 1)	33.4997(1, 1)	30.2056(1, 1)	27.4195(1, 1)
			115.2486(1, 2)	98.3354(1, 2)	88.7494(1, 2)	80.3378(1, 2)
			145.8366(1, 3)	130.9174(1, 3)	121.3814(1, 3)	109.7351(1, 3)
		0.7	36.0654(1, 1)	30.5761(1, 1)	27.5611(1, 1)	25.0445(1, 1)
			133.5838(1, 2)	113.5649(1, 2)	102.3231(1, 2)	92.6019(1, 2)
			151.7192(1, 3)	136.3369(1, 3)	126.5775(1, 3)	114.6753(1, 3)
120	0.1	0.5	3.3755(1, 1)	2.8599(1, 1)	2.5777(1, 1)	2.3432(1, 1)
			22.2070(2, 1)	18.8166(2, 1)	16.9588(2, 1)	15.4143(2, 1)
			45.0449(1, 3)	38.2303(1, 3)	34.4850(1, 3)	31.3441(1, 3)
		0.7	2.7741(1, 1)	2.3501(1, 1)	2.1181(1, 1)	1.9257(1, 1)
			19.2817(2, 1)	16.3321(2, 1)	14.7184(2, 1)	13.3804(2, 1)
			46.9451(3, 1)	39.7699(3, 1)	35.8416(3, 1)	32.5806(3, 1)
	0.2	0.5	3.3302(1, 1)	2.8236(1, 1)	2.5455(1, 1)	2.3134(1, 1)
			16.0149(1, 2)	14.3716(1, 2)	13.3184(1, 2)	12.0317(1, 2)
			42.4716(1, 3)	36.1541(1, 3)	32.6358(1, 3)	29.6223(1, 3)
		0.7	2.7463(1, 1)	2.3281(1, 1)	2.0987(1, 1)	1.9077(1, 1)
			13.1631(1, 2)	11.8122(1, 2)	10.9463(1, 2)	9.8883(1, 2)
			46.2405(3, 1)	39.2118(3, 1)	35.3472(3, 1)	32.1161(3, 1)
240	0.1	0.5	0.9764(1, 1)	0.8278(1, 1)	0.7464(1, 1)	0.6785(1, 1)
			3.3755(2, 1)	2.8600(2, 1)	2.5777(2, 1)	2.3432(2, 1)
			11.3135(3, 1)	9.5850(3, 1)	8.6385(3, 1)	7.8525(3, 1)
		0.7	0.7598(1, 1)	0.6441(1, 1)	0.5807(1, 1)	0.5279(1, 1)
			2.7741(2, 1)	2.3501(2, 1)	2.1181(2, 1)	1.9256(2, 1)
			9.5809(3, 1)	8.1154(3, 1)	7.3136(3, 1)	6.6489(3, 1)
	0.2	0.5	0.9537(1, 1)	0.8097(1, 1)	0.7305(1, 1)	0.6639(1, 1)
			3.3302(2, 1)	2.8236(2, 1)	2.5455(2, 1)	2.3134(2, 1)
			11.1417(3, 1)	9.4474(3, 1)	8.5159(3, 1)	7.7374(3, 1)
		0.7	0.7442(1, 1)	0.6317(1, 1)	0.5698(1, 1)	0.5179(1, 1)
			2.7463(2, 1)	2.3281(2, 1)	2.0987(2, 1)	1.9078(2, 1)
			9.5049(3, 1)	8.0549(3, 1)	7.2603(3, 1)	6.5993(3, 1)
360	0.1	0.5	1.3427(1, 1)	1.1389(1, 1)	1.0271(1, 1)	0.9337(1, 1)
			3.3755(3, 1)	2.8599(3, 1)	2.5777(3, 1)	2.3433(3, 1)
			10.8118(1, 2)	9.7022(1, 2)	8.9910(1, 2)	8.1220(1, 2)
		0.7	1.0138(1, 1)	0.8598(1, 1)	0.7753(1, 1)	0.7048(1, 1)
			2.7741(3, 1)	2.3501(3, 1)	2.1181(3, 1)	1.9256(3, 1)
			8.6234(1, 2)	7.7384(1, 2)	7.1712(1, 2)	6.4782(1, 2)
	0.2	0.5	1.2995(1, 1)	1.1045(1, 1)	0.9969(1, 1)	0.9060(1, 1)
			3.3302(3, 1)	2.8236(3, 1)	2.5455(3, 1)	2.3134(3, 1)
			5.4059(1, 2)	4.8512(1, 2)	4.4956(1, 2)	4.0611(1, 2)
		0.7	0.9858(1, 1)	0.8375(1, 1)	0.7558(1, 1)	0.6869(1, 1)
			2.7463(3, 1)	2.3281(3, 1)	2.0987(3, 1)	1.9077(3, 1)
			4.3117(1, 2)	3.8692(1, 2)	3.5856(1, 2)	3.2391(1, 2)

$$
\begin{aligned}
&+\frac{k^2A_{33}\lambda_3-I_0\omega_m^2}{k^2A_{33}}\left(C_5J_{\mu_m}\left(\sqrt{\lambda_3}r\right)+C_6Y_{\mu_m}\left(\sqrt{\lambda_3}r\right)\right),\\
\psi_{rm}=&\frac{\mu_mB_{33}I_0-\mu_mA_{33}I_1}{O_6r}\varphi_2(r)+\frac{B_{33}I_1\mu_m+D_{33}I_0\mu_m}{O_6r}\left(C_9I_{\mu_m}(\lambda_5r)+C_{10}K_{\mu_m}(\lambda_5r)\right)\\
&+\frac{k^2A_{33}I_0\mu_m}{O_6r}\left(C_1I_{\mu_m}\left(\sqrt{-\lambda_1}r\right)+C_2K_{\mu_m}\left(\sqrt{-\lambda_1}r\right)\right)\\
&+\frac{k^2A_{33}I_0\sqrt{-\lambda_1}}{O_6}\left(C_1I_{\mu_m+1}\left(\sqrt{-\lambda_1}r\right)+C_2K_{\mu_m+1}\left(\sqrt{-\lambda_1}r\right)\right)\\
&+\frac{k^2A_{33}I_0\mu_m}{O_6r}\left(C_3J_{\mu_m}\left(\sqrt{\lambda_2}r\right)+C_4Y_{\mu_m}\left(\sqrt{\lambda_2}r\right)\right)
\end{aligned}
$$

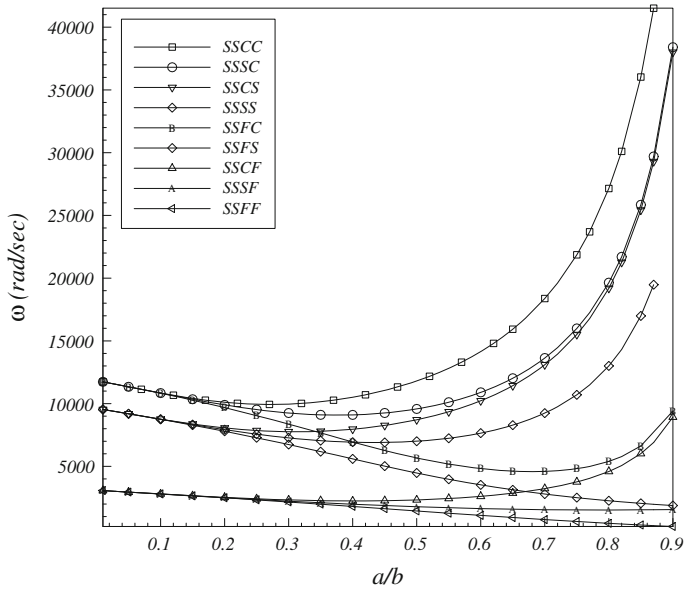

Fig. 2 The variation of the first natural frequency of an FG annular sector plate versus the aspect ratio for all possible boundary conditions ($h/c = 0.1$, $n = 0.5$, $\beta = 60°$)

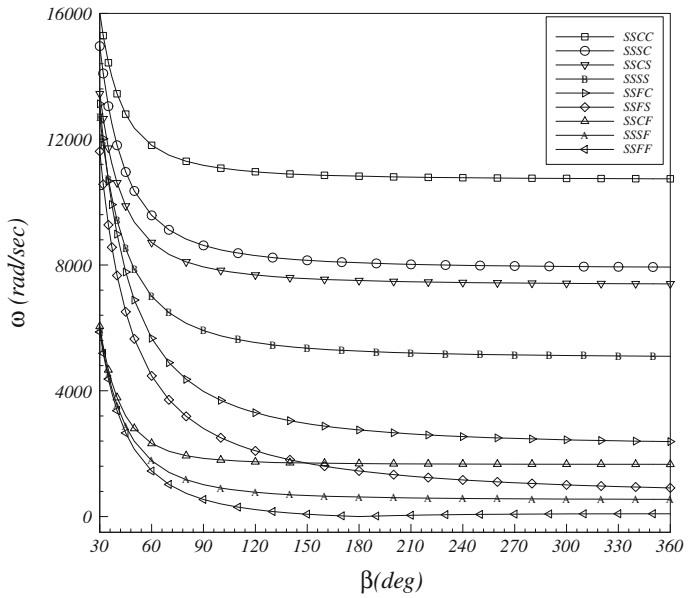

Fig. 3 The variation of the first natural frequency of an FG annular sector plate versus the sector angle for all possible boundary conditions ($h/c = 0.1$, $n = 0.5$, $a/b = 0.5$)

$$
\begin{aligned}
&+\frac{k^2 A_{33} I_0 \mu_m}{O_6 r}\left(C_5 J_{\mu_m}\left(\sqrt{\lambda_3} r\right)+C_6 Y_{\mu_m}\left(\sqrt{\lambda_3} r\right)\right)\\
&+\frac{-B_{33} I_1 \mu_m+D_{33} I_0 \mu_m}{O_6 r}\left(C_7 J_{\mu_m}(\lambda_4 r)+C_8 Y_{\mu_m}(\lambda_4 r)\right)\\
&+\frac{k^2 A_{33} I_0 \sqrt{\lambda_2}}{O_6}\left(C_3 J_{\mu_m+1}\left(\sqrt{\lambda_2} r\right)+C_4 Y_{\mu_m+1}\left(\sqrt{\lambda_2} r\right)\right)\\
&+\frac{k^2 A_{33} I_0 \sqrt{\lambda_3}}{O_6}\left(C_5 J_{\mu_m+1}\left(\sqrt{\lambda_3} r\right)+C_6 Y_{\mu_m+1}\left(\sqrt{\lambda_3} r\right)\right),
\end{aligned}
$$

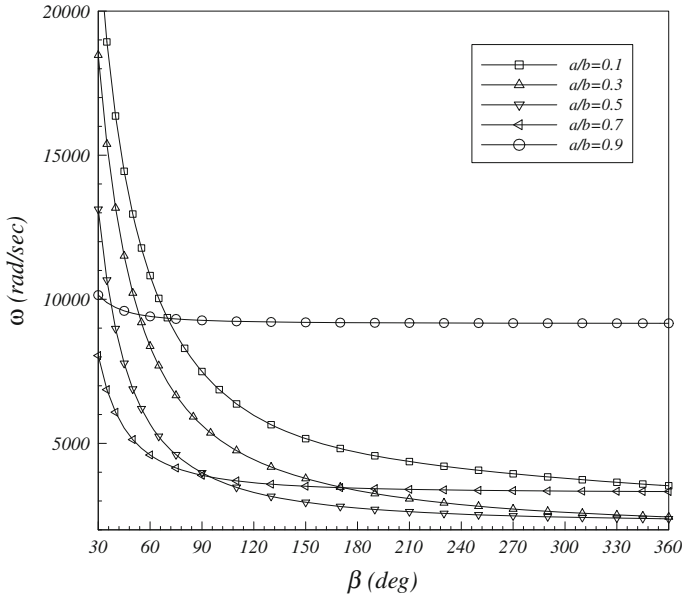

Fig. 4 The variation of the first natural frequency of an FG annular sector plate versus the sector angle and aspect ratio for *SSFC* boundary condition ($h/c = 0.1, n = 0.5$)

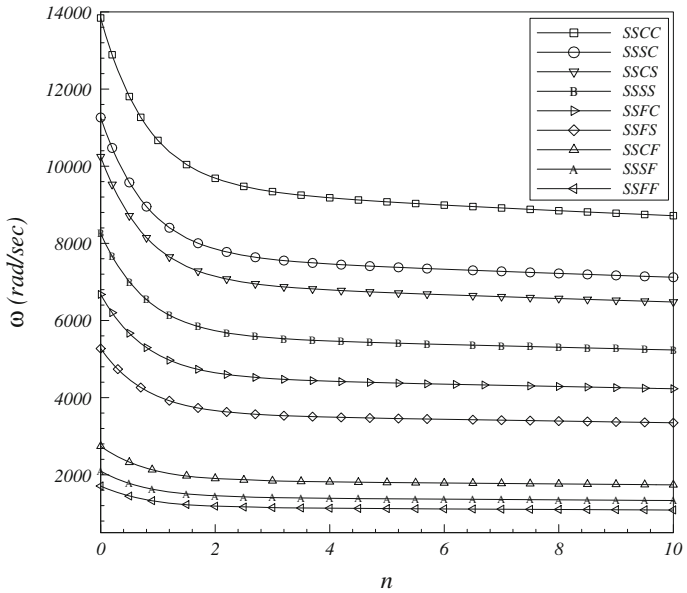

Fig. 5 The variation of the first natural frequency of an FG annular sector plate versus the power law index for all possible boundary conditions ($h/c = 0.1, a/b = 0.5, \beta = 60°$)

$$
\begin{aligned}
\psi_{\theta m} = & \frac{(A_{11}I_1 - B_{11}I_0)\mu_m}{O_6 r}\varphi_1(r) + \frac{(B_{11}I_1 - D_{11}I_0)\mu_m}{O_6 r}\varphi_3(r) \\
& + \frac{D_{33}I_0\mu_m - B_{33}I_1\mu_m}{O_6 r}\left(C_9 I_{\mu_m}(\lambda_5 r) + C_{10}K_{\mu_m}(\lambda_5 r)\right) \\
& + \frac{k^2 A_{33}I_0\mu_m}{O_6 r}\left(C_1 I_{\mu_m}\left(\sqrt{-\lambda_1}r\right) + C_2 K_{\mu_m}\left(\sqrt{-\lambda_1}r\right)\right) \\
& + \frac{(D_{33}I_0 - B_{33}I_1)\lambda_5}{O_6}\left(C_9 I_{\mu_m+1}(\lambda_5 r) + C_{10}K_{\mu_m+1}(\lambda_5 r)\right)
\end{aligned}
$$

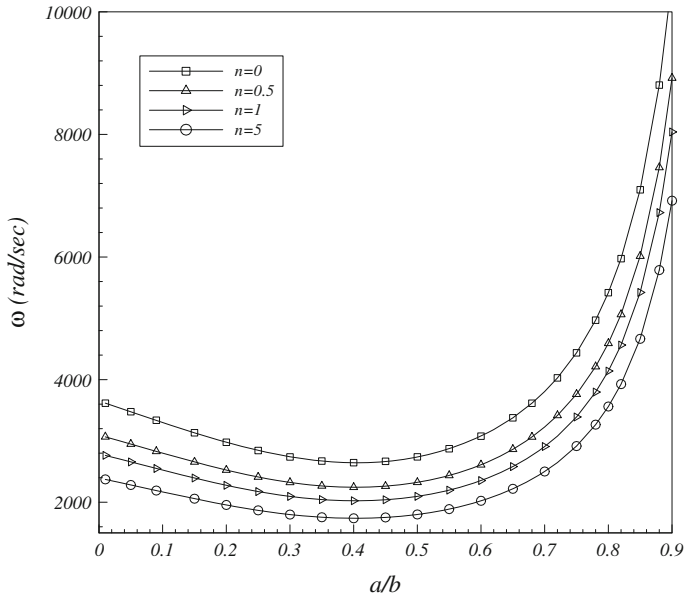

Fig. 6 The variation of the first natural frequency of an FG annular sector plate versus the sector angle and power law index for *SSCF* boundary condition ($h/c = 0.1, n = 0.5$)

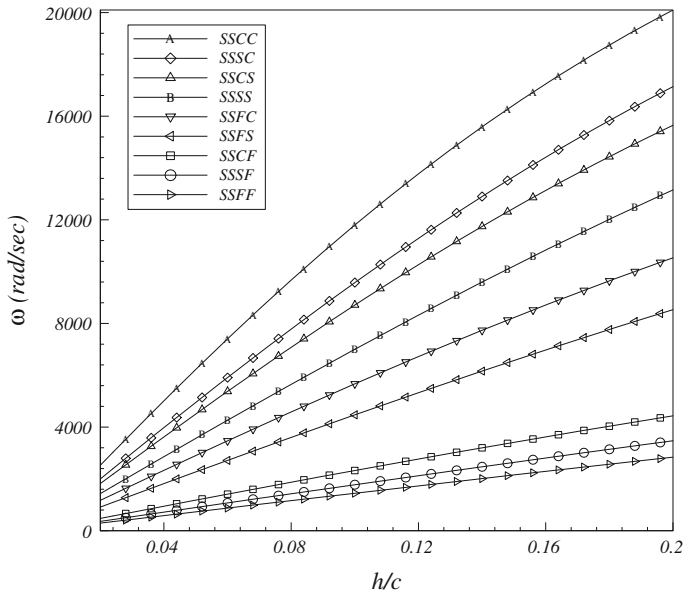

Fig. 7 The variation of the first natural frequency of an FG annular sector plate versus the thickness/difference radiuses ratio for all possible boundary conditions ($a/b = 0.5, n = 0.5, \beta = 60°$)

$$
\begin{aligned}
&+\frac{k^2 A_{33} I_0 \mu_m}{O_6 r}\left(C_3 J_{\mu_m}\left(\sqrt{\lambda_2} r\right)+C_4 Y_{\mu_m}\left(\sqrt{\lambda_2} r\right)\right)\\
&+\frac{k^2 A_{33} I_0 \mu_m}{O_6 r}\left(C_5 J_{\mu_m}\left(\sqrt{\lambda_3} r\right)+C_6 Y_{\mu_m}\left(\sqrt{\lambda_3} r\right)\right)\\
&+\frac{(D_{33} I_0-B_{33} I_1)\mu_m}{O_6 r}\left(C_7 J_{\mu_m}(\lambda_4 r)+C_8 Y_{\mu_m}(\lambda_4 r)\right)\\
&+\frac{(B_{33} I_1-D_{33} I_0)\lambda_4}{O_6}\left(C_7 J_{\mu_m+1}(\lambda_4 r)+C_8 Y_{\mu_m+1}(\lambda_4 r)\right),
\end{aligned}
$$

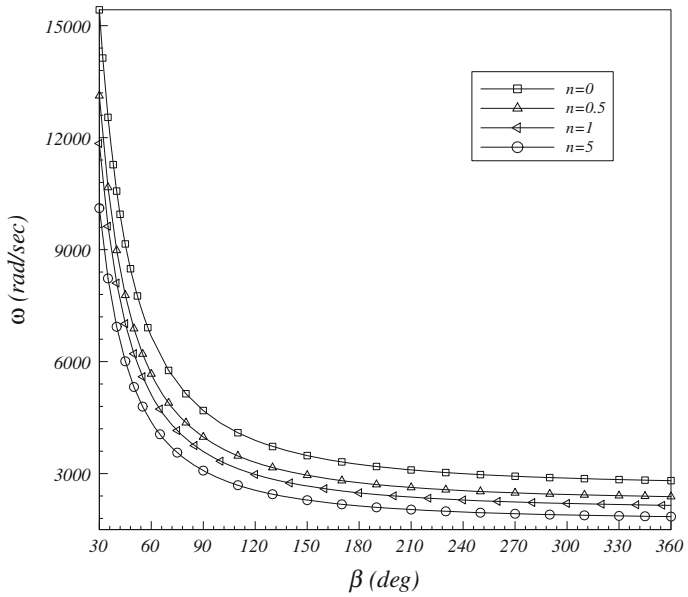

Fig. 8 The variation of the first natural frequency of an FG annular sector plate versus the sector angle and power law index for *SSFC* boundary condition ($h/c = 0.1$, $a/b = 0.5$)

$$
\begin{aligned}
u_{1m} = &-\frac{O_4\mu_m}{O_5 r}\left(C_9 I_{\mu_m}(\lambda_5 r) + C_{10} K_{\mu_m}(\lambda_5 r)\right)\\
&-\frac{k^2 A_{33} I_1 \omega_m^2 \mu_m}{O_5 r}\left(C_1 I_{\mu_m}\left(\sqrt{-\lambda_1} r\right) + C_2 K_{\mu_m}\left(\sqrt{-\lambda_1} r\right)\right)\\
&-\frac{k^2 A_{33} I_1 \omega_m^2 \sqrt{-\lambda_1}}{O_5}\left(C_1 I_{\mu_m+1}\left(\sqrt{-\lambda_1} r\right) + C_2 K_{\mu_m+1}\left(\sqrt{-\lambda_1} r\right)\right)\\
&-\frac{k^2 A_{33} I_1 \omega_m^2 \mu_m}{O_5 r}\left(C_3 J_{\mu_m}\left(\sqrt{\lambda_2} r\right) + C_4 Y_{\mu_m}\left(\sqrt{\lambda_2} r\right)\right)\\
&-\frac{O_4\mu_m}{O_5 r}\left(C_7 J_{\mu_m}(\lambda_4 r) + C_8 Y_{\mu_m}(\lambda_4 r)\right)\\
&+\frac{k^2 A_{33} I_1 \omega_m^2 \sqrt{\lambda_2}}{O_5}\left(C_1 J_{\mu_m+1}\left(\sqrt{\lambda_2} r\right) + C_2 Y_{\mu_m+1}\left(\sqrt{\lambda_2} r\right)\right)\\
&+\frac{k^2 A_{33} I_1 \omega_m^2 \sqrt{\lambda_3}}{O_5}\left(C_1 J_{\mu_m+1}\left(\sqrt{\lambda_3} r\right) + C_2 Y_{\mu_m+1}\left(\sqrt{\lambda_3} r\right)\right) - \frac{O_2\mu_m}{O_5 r}\varphi_2(r),\\
u_{2m} = &-\frac{O_4\alpha}{O_5 r}\left(C_9 I_{\mu_m}(\lambda_5 r) + C_{10} K_{\mu_m}(\lambda_5 r)\right) - \frac{k^2 A_{33} I_1 \omega_m^2 \mu_m}{O_5 r}\left(C_1 I_{\mu_m}\left(\sqrt{-\lambda_1} r\right) + C_2 K_{\mu_m}\left(\sqrt{-\lambda_1} r\right)\right)\\
&-\frac{O_4\lambda_5}{O_5}\left(C_9 I_{\mu_m+1}\left(\sqrt{\lambda_5} r\right) + C_{10} K_{\mu_m+1}\left(\sqrt{\lambda_5} r\right)\right) - \frac{k^2 A_{33} I_1 \omega_m^2 \mu_m}{O_5 r}\left(C_3 J_{\mu_m}\left(\sqrt{\lambda_2} r\right)\right.\\
&\left.+ C_4 Y_{\mu_m}\left(\sqrt{\lambda_2} r\right)\right) - \frac{k^2 A_{33} I_1 \omega_m^2 \mu_m}{O_5 r}\left(C_5 J_{\mu_m}\left(\sqrt{\lambda_3} r\right) + C_6 Y_{\mu_m}\left(\sqrt{\lambda_3} r\right)\right) - \frac{O_4\mu_m}{O_5 r}\left(C_7 I_{\mu_m}(\lambda_4 r)\right.\\
&\left.+ C_8 K_{\mu_m}(\lambda_4 r)\right) + \frac{O_4\lambda_5}{O_5}\left(C_7 I_{\mu_m+1}(\lambda_4 r) + C_8 K_{\mu_m+1}(\lambda_4 r)\right) + \frac{O_1\mu_m}{O_5 r}\varphi_1(r) + \frac{O_3\mu_m}{O_5 r}\varphi_3(r) \qquad \text{(A.1)}
\end{aligned}
$$

where

$$
\begin{aligned}
O_1 &= \left(k^2 A_{33} - I_2\omega_m^2\right) A_{11} + B_{11} I_1 \omega_m^2,\\
O_2 &= \left(k^2 A_{33} - I_2\omega_m^2\right) A_{33} + B_{33} I_1 \omega_m^2,\\
O_3 &= \left(k^2 A_{33} - I_2\omega_m^2\right) B_{11} + D_{11} I_1 \omega_m^2,
\end{aligned}
$$

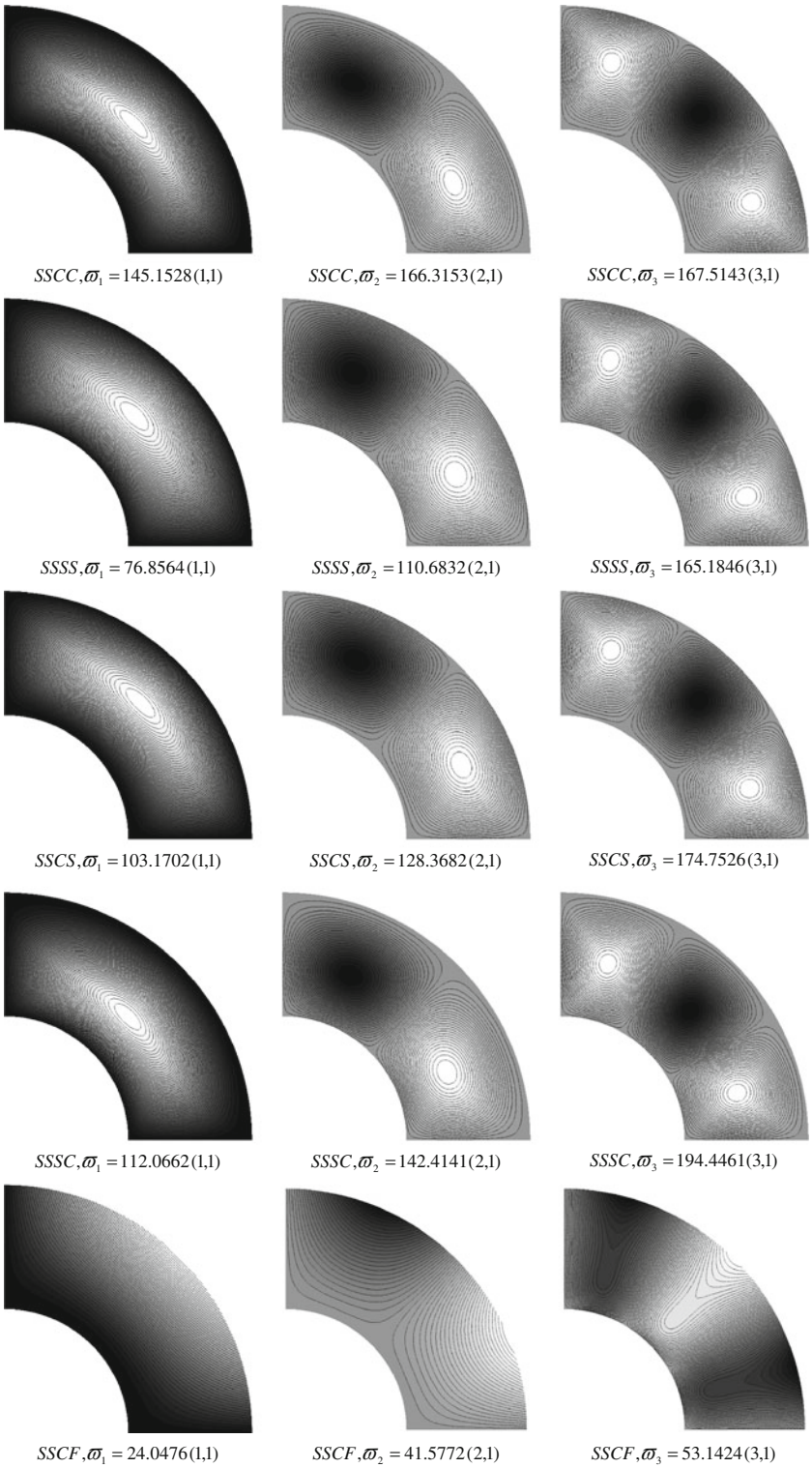

Fig. 9 Mode shape plots of the annular sector plate for all possible boundary conditions ($n = 0.5$, $h/c = 0.1$, $a/b = 0.5$, $\beta = 90°$)

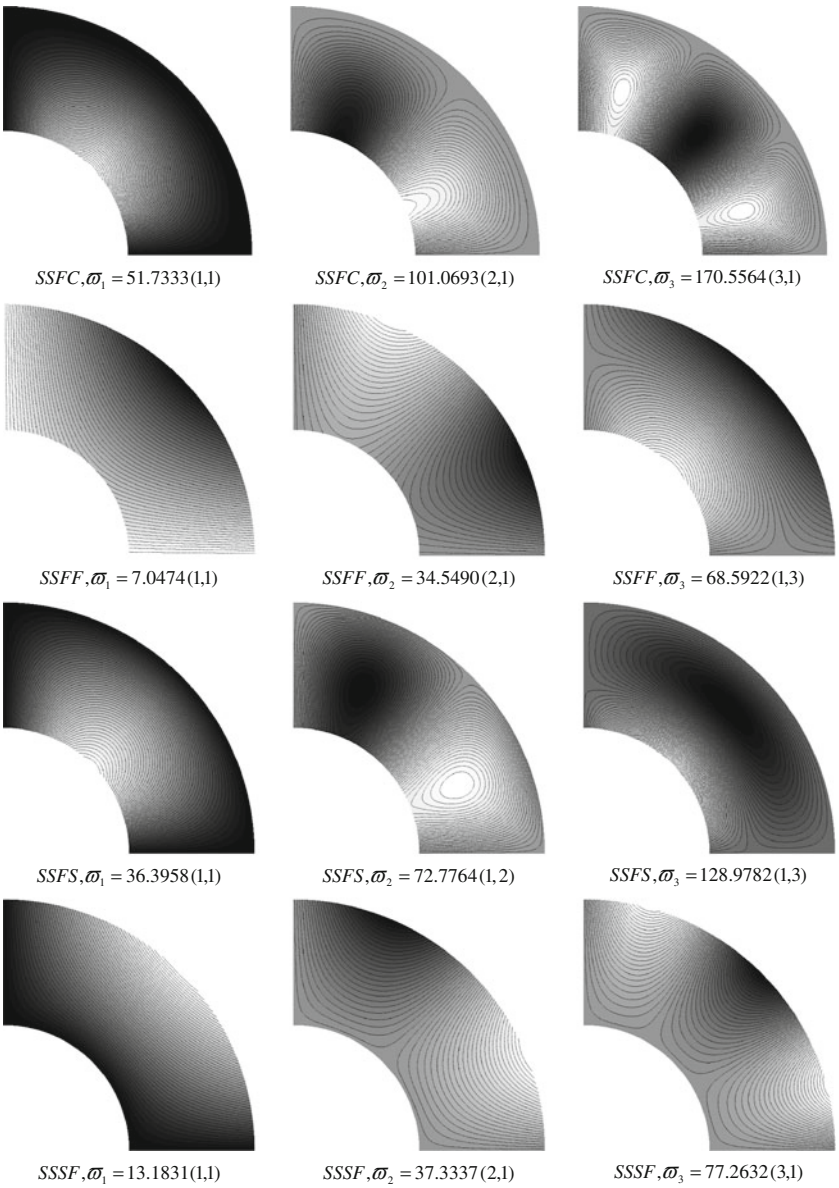

Fig. 9 continued

$$
\begin{aligned}
O_4 &= \left(k^2 A_{33} - I_2 \omega_m^2\right) B_{33} + D_{33} I_1 \omega_m^2, \\
O_5 &= -\left(I_1^2 \omega_m^4 + I_0 \omega_m^2 \left(k^2 A_{33} - I_2 \omega_m^2\right)\right), \\
O_6 &= O_5 \big/ \omega_m^2, \\
K_1 &= \frac{\hat{D} I_0}{k^2 A_{33} J_1} + \frac{J_2}{J_1}, \\
K_2 &= \frac{I_0}{J_1} - \frac{I_0 J_2 \omega_m^2}{k^2 A_{33} J_1}.
\end{aligned}
\tag{A.2}
$$

References

1. Koizumi, M.: FGM activities in Japan. Compos. Part B. **28**, 1–4 (1997)
2. Reddy, J.N.: Analysis of functionally graded plates. Int. J. Num. Meth. Eng. **47**, 663–684 (2000)

3. Srinivasan, R.S., Thiruvekatachari, V.: Free vibration of transverse isotropic annular sector Mindlin plates. J. Sound Vib. **101**, 193–201 (1985)
4. Cheung, Y.K., Kwok, W.L.: Dynamic analysis of circular and sector thick, layered plates. J. Sound Vib. **42**, 147–158 (1975)
5. Mizusawa, T.: Vibration of thick annular sector plates using semi-analytical methods. J. Sound Vib. **150**, 245–259 (1991)
6. Xiang, Y., Liew, K.M., Kitipornchai, S.: Transverse vibration of thick annular sector plates. ASCE, J. Eng. Mech. **119**, 1579–1599 (1993)
7. McGee, O.G., Leissa, A.W., Huang, C.S.: Vibration of completely free sectorial plates. J. Sound Vib. **164**, 565–569 (1993)
8. McGee, O.G., Huang, C.S., Leissa, A.W.: Comprehensive exact solutions for free vibrations of thick annular sectorial plates with simply supported radial edges. Int. J. Mech. Sci. **37**, 537–566 (1995)
9. Huang, C.S., McGee, O.G., Leissa, A.W.: Exact analytical solutions for free vibrations of thick sectorial plates with simply supported radial edges. Int. J. Solids Struct. **31**, 1609–1631 (1994)
10. Liew, K.M., Liu, F.L.: Differential quadrature method for vibration analysis of shear deformable annular sector plates. J. Sound Vib. **230**, 335–356 (2000)
11. Wang, X., Wang, Y.: Free vibration analyses of thin sector plates by the new version of differential quadrature method. Com. Meth. Appl. Mech. Eng. **193**, 3957–3971 (2004)
12. Yongqiang, L., Jian, L.: Free vibration analysis of circular and annular sectorial thin plates using curve strip Fourier p-element. J. Sound Vib. **305**, 457–466 (2007)
13. Chen, W.Q., Ding, H.J.: On free vibration of a functionally graded piezoelectric rectangular plate. Acta Mech. **153**, 207–216 (2002)
14. Zhou, D., Lo, S.H., Cheung, Y.K.: 3-D vibration analysis of annular sector plates using the Chebyshev–Ritz method. J. Sound Vib. **320**, 421–437 (2009)
15. Jomehzadeh, E., Saidi, A.R.: Analytical solution for free vibration of transversely isotropic sector plates using a boundary layer function. Thin-Walled Struct. **47**, 82–88 (2009)
16. Jomehzadeh, E., Saidi, A.R.: Accurate natural frequencies of transversely isotropic moderately thick annular sector plates. J. Mech. Eng. Sci. Proc. IMechE, Part C. **223**, 307–317 (2009)
17. Srinivasan, R.S., Thiruvekatachari, V.: Free vibration analysis of laminated annular sector plates. J. Sound Vib. **109**, 89–96 (1986)
18. Atashipour, S.R., Saidi, A.R., Jomehzadeh, E.: On the boundary layer phenomenon in bending of thick annular sector plates using third-order shear deformation theory. Acta Mech. **211**, 89–99 (2010)
19. Huang, C.S., Ho, K.H.: An analytical solution for vibrations of a polarly orthotropic Mindlin sectorial plate with simply supported radial edges. J. Sound Vib. **273**, 277–294 (2004)
20. Sharma, A., Sharda, H.B., Nath, Y.: Stability and vibration of thick laminated composite sector plates. J. Sound Vib. **287**, 1–23 (2005)
21. Nosier, A., Yavari, A., Sarkani, S.: On a boundary layer phenomenon in Mindlin-Reissner plate theory for laminated circular sector plates. Acta Mech. **151**, 149–161 (2001)
22. Malekzadeh, P.: Three-dimensional free vibration analysis of thick laminated annular sector plates using a hybrid method. Compos. Struct. **90**, 428–437 (2009)
23. Malekzadeh, P., Golbahar Haghighi, M.R., Gholami, M.: Dynamic response of thick laminated annular sector plates subjected to moving load. Compos. Struct. **92**, 155–163 (2010)
24. Malekzadeh, P., Afsari, A., Zahedinejad, P., Bahadori, R.: Three-dimensional layer wise-finite element free vibration analysis of thick laminated annular plates on elastic foundation. Appl. Math. Model. **34**, 776–790 (2010)
25. Nie, G.J., Zhong, Z.: Vibration analysis of functionally graded annular sectorial plates with simply supported radial edges. Compos. Struct. **84**, 167–176 (2008)
26. Hosseini-Hashemi, Sh., Akhavan, H., Rokni Damavandi Taher, H., Daemi, N., Alibeigloo, A.: Differential quadrature analysis of functionally graded circular and annular sector plates on elastic foundation. Mat. Des. **31**, 1871–1880 (2010)
27. Hosseini-Hashemi, Sh., Rokni Damavandi Taher, H., Akhavan, H.: Vibration analysis of radially FGM sectorial plates of variable thickness on elastic foundations. Compos. Struct. **92**, 1734–1743 (2010)
28. Reddy, J.N.: Theory and Analysis of Elastic Plates and Shells. 2nd edn. CRC Press, Philadelphia (2007)
29. Hasani Baferani, A., Saidi, A.R., Jomehzadeh, E.: An exact solution for free vibration of thin functionally graded rectangular plates. IMechE, J. Mech. Eng. Sci. Part: C. doi:10.1243/09544062JMES2171 (in press)
30. Nosier, A., Fallah, F.: Reformulation of Mindlin-Reissner governing equations of functionally graded circular plates. Acta Mech. **198**, 209–233 (2008)
31. Irschik, H.: On vibrations of layered beams and plates. Zeitschrift für Angewandte Mathematik und Mechanik (ZAMM) **73**, 34–45 (1993)
32. Naderi, A., Saidi, A.R.: On pre-buckling configuration of functionally graded Mindlin rectangular plates. Mech. Res. Commun. **37**, 535–538 (2010)